

## CHAPTER IV

### RESULTS AND DISCUSSIONS

#### Polarizing Microscope Investigation

##### Potassium Chromate

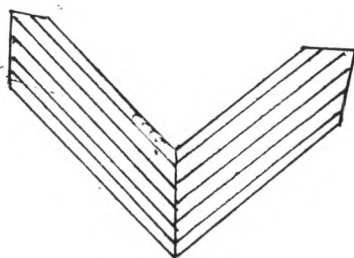
Potassium chromate was viewed in plane polarized light. It was orthorhombic, yellow colour. As it was rotated, showed no change in appearance. Then it was viewed between crossed polars, it showed light or colour against the dark ground, and as it was rotated, changed alternately between light and dark every  $90^{\circ}$  rotation. This confirmed that it was anisotropic.

##### Potassium Sulphate

It was orthorhombic, colourless. It showed the same phenomena as potassium chromate.

##### Mixed Crystals Potassium Chromate/ Potassium Sulphate.

The mixed crystals were orthorhombic, yellow colour. Some of the mixed crystals showed twinning( they consisted of two individuals grown together in some definite orientation). The appearance of the mixed crystals were similar to pure crystals.



Twinning in mixed crystals

## The Composition of Mixed Crystals

### 1. The Homogeneity of the Mixed Crystals.

The crystal homogeneity was a consideration in this study, it was checked by randomly sampling and analysing the composition of the mixed crystals in each sample. The replicate determinations of the composition of sample were performed 10 times at random. The data obtained was reported in Table 9. The standard deviation was calculated by the formula:

$$\delta = \pm \sqrt{\frac{\sum (x - \bar{x})^2}{N}}$$

where  $x$  = individual value

$\bar{x}$  = mean value

$N$  = number of samplings

Table 9. The composition of mixed crystal sample obtained from 10 samplings at random.

Number of sampling (N= 10)	Composition of mixed crystal			
	Potassium chromate		Potassium sulphate	
	% by weight	Mole fraction	% by weight	Mole fraction
1	26.12	0.2409	74.39	0.7639
2	25.65	0.2364	74.80	0.7678
3	26.70	0.2464	72.11	0.7423
4	26.33	0.2429	72.04	0.7416
5	27.38	0.2528	70.43	0.7263
6	26.50	0.2445	73.66	0.7570
7	27.11	0.2503	73.89	0.7592
8	26.98	0.2490	70.05	0.7227
9	26.41	0.2436	74.12	0.7614
10	25.12	0.2314	74.20	0.7621
average ( $\bar{x}$ )	26.43	0.2438	72.97	0.7504
standard deviation ( $\delta$ )	0.63	0.0061	1.62	0.0153

The mixed crystal samples were analyzed and the composition of the mixed crystals were evaluated by the above procedure and summarized in Table 10.

Table 10. The composition of the mixed crystals.

Number sample	Composition of the mixed crystals			
	Potassium chromate		Potassium sulphate	
	% by weight	Mole fraction	% by weight	Mole fraction
	$\bar{x} \pm \delta$	$\bar{x} \pm \delta$	$\bar{x} \pm \delta$	$\bar{x} \pm \delta$
1	1.28 $\pm$ 0.20	0.0115 $\pm$ 0.0014	96.67 $\pm$ 0.44	0.9700 $\pm$ 0.0035
2	2.15 $\pm$ 0.68	0.0193 $\pm$ 0.0062	95.55 $\pm$ 0.72	0.9599 $\pm$ 0.0063
3	2.56 $\pm$ 0.31	0.0230 $\pm$ 0.0028	95.00 $\pm$ 0.59	0.9549 $\pm$ 0.0044
4	4.38 $\pm$ 0.23	0.0395 $\pm$ 0.0021	94.64 $\pm$ 0.70	0.9516 $\pm$ 0.0061
5	6.61 $\pm$ 0.29	0.0597 $\pm$ 0.0027	93.38 $\pm$ 0.34	0.9401 $\pm$ 0.0025
6	13.41 $\pm$ 1.74	0.1220 $\pm$ 0.0161	85.67 $\pm$ 0.98	0.8695 $\pm$ 0.0090
7	26.43 $\pm$ 0.63	0.2438 $\pm$ 0.0061	72.97 $\pm$ 1.62	0.7504 $\pm$ 0.0153
8	52.00 $\pm$ 0.91	0.4930 $\pm$ 0.0090	47.51 $\pm$ 1.10	0.5021 $\pm$ 0.0102
9	62.56 $\pm$ 1.01	0.6000 $\pm$ 0.0100	36.44 $\pm$ 1.31	0.3898 $\pm$ 0.0127
10	77.95 $\pm$ 0.87	0.7604 $\pm$ 0.0082	20.42 $\pm$ 1.84	0.2223 $\pm$ 0.0179
11	82.30 $\pm$ 1.96	0.8067 $\pm$ 0.0191	17.13 $\pm$ 1.03	0.1872 $\pm$ 0.0098
12	88.46 $\pm$ 1.24	0.8731 $\pm$ 0.0122	9.62 $\pm$ 1.56	0.0974 $\pm$ 0.0144
13	91.68 $\pm$ 1.95	0.9082 $\pm$ 0.0188	7.21 $\pm$ 0.70	0.0797 $\pm$ 0.0061
14	95.84 $\pm$ 0.92	0.9319 $\pm$ 0.0086	4.48 $\pm$ 0.54	0.0497 $\pm$ 0.0042

2. The Comparison of Three Analysis Method of Potassium Chromate in the Mixed Crystals

The concentration of potassium chromate obtained from three methods : Iodometric titration, ferrous sulphate titration and spectrophotometric method, were compared in Table 11.

Table 11. The comparison of three methods analysing the concentration of potassium chromate in the mixed crystals.

Number of sample	% by weight of $K_2CrO_4$ in mixed crystals		
	Iodometric method	Ferrous sulphate method	Spectrophotometric method
	$\bar{x} \pm \frac{6}{6}$	$\bar{x} \pm \frac{6}{6}$	$\bar{x} \pm \frac{6}{6}$
1	1.28 $\pm$ 0.20	1.37 $\pm$ 0.47	1.55 $\pm$ 0.39
2	2.15 $\pm$ 0.18	2.94 $\pm$ 0.23	2.68 $\pm$ 0.16
3	3.56 $\pm$ 0.32	2.65 $\pm$ 0.27	3.04 $\pm$ 0.35
4	4.38 $\pm$ 0.23	4.68 $\pm$ 0.28	5.69 $\pm$ 0.30
5	6.61 $\pm$ 0.29	6.76 $\pm$ 0.44	9.00 $\pm$ 0.40
6	13.41 $\pm$ 1.74	13.85 $\pm$ 1.85	16.07 $\pm$ 1.07
7	26.43 $\pm$ 0.63	26.66 $\pm$ 1.57	28.99 $\pm$ 1.65
8	52.00 $\pm$ 0.91	55.61 $\pm$ 1.82	56.11 $\pm$ 1.21
9	62.56 $\pm$ 1.01	64.68 $\pm$ 2.88	66.02 $\pm$ 0.68
10	77.95 $\pm$ 0.87	79.62 $\pm$ 1.99	75.42 $\pm$ 1.99
11	82.30 $\pm$ 1.96	84.34 $\pm$ 1.86	84.35 $\pm$ 2.44
12	88.46 $\pm$ 1.25	89.31 $\pm$ 2.14	89.93 $\pm$ 2.99
13	91.68 $\pm$ 1.94	93.01 $\pm$ 2.22	95.26 $\pm$ 2.32
14	93.84 $\pm$ 0.92	95.66 $\pm$ 2.67	94.08 $\pm$ 3.04

### 3. The Reproducibility of Crystallization of the Mixed Crystals.

The reproducibility of crystallization of the mixed crystals was also considered to see how the composition of the mixed crystals depended on the composition of the crystallising solution. The mixed crystals which were crystallized from separate crystallising solutions of the same composition were analyzed and the results of the composition of the mixed crystals were reported in Table 12 .

Table 12. The composition of the mixed crystals which were crystallized from separate crystallising solutions of the same composition.

Mole Fraction	Number of experiment			
	1	2	3	4
$K_2CrO_4$ in solution	0.1110	0.1110	0.1110	0.1110
in the mixed crystal	0.0115	0.0142	0.0141	0.0133
$K_2SO_4$ in solution	0.8890	0.8890	0.8890	0.8890
in the mixed crystal	0.9714	0.9785	0.9863	0.9700
$K_2CrO_4$ in solution	0.2500	0.2500	0.2500	0.2500
in the mixed crystal	0.0193	0.0188	0.0198	0.0175
$K_2SO_4$ in solution	0.7500	0.7500	0.7500	0.7500
in the mixed crystal	0.9599	0.9640	0.9734	0.9516
$K_2CrO_4$ in solution	0.4975	0.4975	0.4975	0.4975
in the mixed crystal	0.0230	0.0251	0.0267	0.0234
$K_2SO_4$ in solution	0.5025	0.5025	0.5025	0.5025
in the mixed crystal	0.9549	0.9511	0.9476	0.9615

Table 12 The composition of the mixed crystals which were  
(cont) crystallized from separate crystallising solutions of  
the same composition .

Mole fraction	Number of experi- ment	1	2	3	4
$K_2CrO_4$ in solution		0.6000	0.6000	0.6000	0.6000
in the mixed crystal		0.0395	0.0341	0.0379	0.0313
$K_2SO_4$ in solution		0.4000	0.4000	0.4000	0.4000
in the mixed crystal		0.9516	0.9474	0.9581	0.9456
$K_2CrO_4$ in solution		0.6667	0.6667	0.6667	0.6667
in the mixed crystal		0.0597	0.0444	0.0513	0.0506
$K_2SO_4$ in solution		0.3333	0.3333	0.3333	0.3333
in the mixed crystal		0.9401	0.9317	0.9386	0.9445
$K_2CrO_4$ in solution		0.8095	0.8095	0.8095	0.8095
in the mixed crystal		0.1220	0.1397	0.1345	0.1118
$K_2SO_4$ in solution		0.1905	0.1905	0.1905	0.1905
in the mixed crystal		0.8695	0.8723	0.8740	0.8712
$K_2CrO_4$ in solution		0.8214	0.8214	0.8214	0.8214
in the mixed crystal		0.2438	0.2410	0.2597	0.2604
$K_2SO_4$ in solution		0.1786	0.1786	0.1786	0.1786
in the mixed crystal		0.7504	0.7438	0.7499	0.7537
$K_2CrO_4$ in solution		0.8889	0.8889	0.8889	0.8889
in the mixed crystal		0.4930	0.5160	0.5049	0.4713
$K_2SO_4$ in solution		0.1111	0.1111	0.1111	0.1111
in the mixed crystal		0.5021	0.4989	0.5048	0.5092

Table 12 The composition of the mixed crystals which were  
(cont) crystallized from separate crystallising solutions of  
the same composition.

Mole fraction	Number of experiment	1	2	3	4
$K_2CrO_4$ in solution		0.9093	0.9093	0.9093	0.9093
	in the mixed crystal	0.6000	0.6238	0.6400	0.6416
$K_2SO_4$ in solution		0.0907	0.0907	0.0907	0.0907
	in the mixed crystal	0.3898	0.3745	0.3852	0.3817
$K_2CrO_4$ in solution		0.9432	0.9432	0.9432	0.9432
	in the mixed crystal	0.7604	0.7732	0.7601	0.7945
$K_2SO_4$ in solution		0.0568	0.0568	0.0568	0.0568
	in the mixed crystal	0.2223	0.2243	0.2296	0.2311
$K_2CrO_4$ in solution		0.9620	0.9620	0.9620	0.9620
	in the mixed crystal	0.8067	0.7900	0.8541	0.8138
$K_2SO_4$ in solution		0.0380	0.0380	0.0380	0.0380
	in the mixed crystal	0.1872	0.1836	0.1749	0.1748
$K_2CrO_4$ in solution		0.9752	0.9752	0.9752	0.9752
	in the mixed crystal	0.8731	0.8535	0.8659	0.8803
$K_2SO_4$ in solution		0.0248	0.0248	0.0248	0.0248
	in the mixed crystal	0.0974	0.0936	0.0896	0.0861
$K_2CrO_4$ in solution		0.9821	0.9821	0.9821	0.9821
	in the mixed crystal	0.9082	0.9014	0.9437	0.9707
$K_2SO_4$ in solution		0.0179	0.0179	0.0179	0.0179
	in the mixed crystal	0.0797	0.0757	0.0735	0.0712
$K_2CrO_4$ in solution		0.9903	0.9903	0.9903	0.9903
	in the mixed crystal	0.9319	0.9517	0.9268	0.9744
$K_2SO_4$ in solution		0.0097	0.0097	0.0097	0.0097
	in the mixed crystal	0.0497	0.0474	0.0694	0.0303

The results in Table 12 showed that the compositions of the mixed crystals depended on the compositions of the crystallizing solutions. Though it was seen that the compositions of the mixed crystals were variable, they depended on the compositions of the crystallizing solutions. The results of this study were different from reference (11) which stated that the concentration of bromate or chlorate ions in  $\text{NaClO}_3/\text{NaBrO}_3$  mixed crystals was almost independent of the solution concentration .

Figure 15 showed mole fraction of potassium chromate in the crystallizing solution and in the mixed crystals while Figure 16 showed those of potassium sulphate.

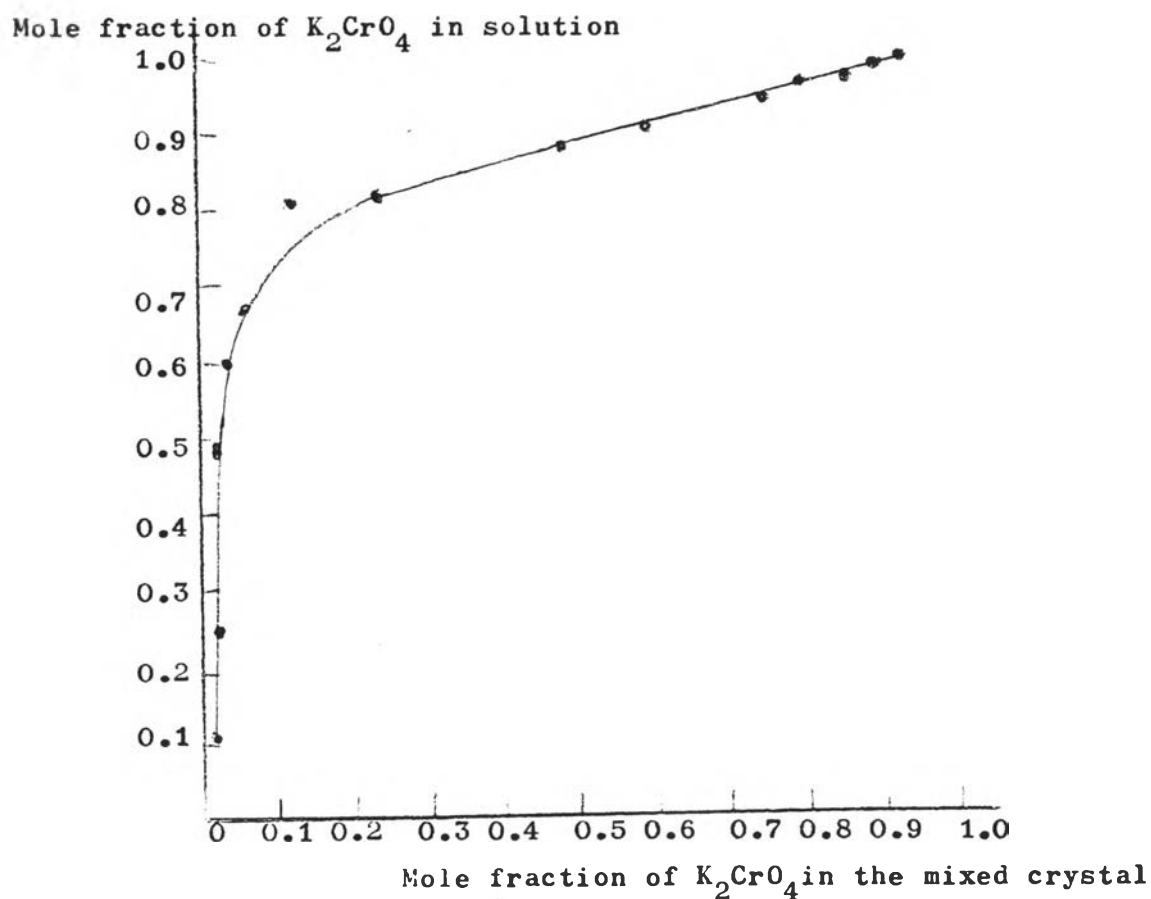


Figure 15. Mole fraction of  $\text{K}_2\text{CrO}_4$  in solution and in the mixed crystal



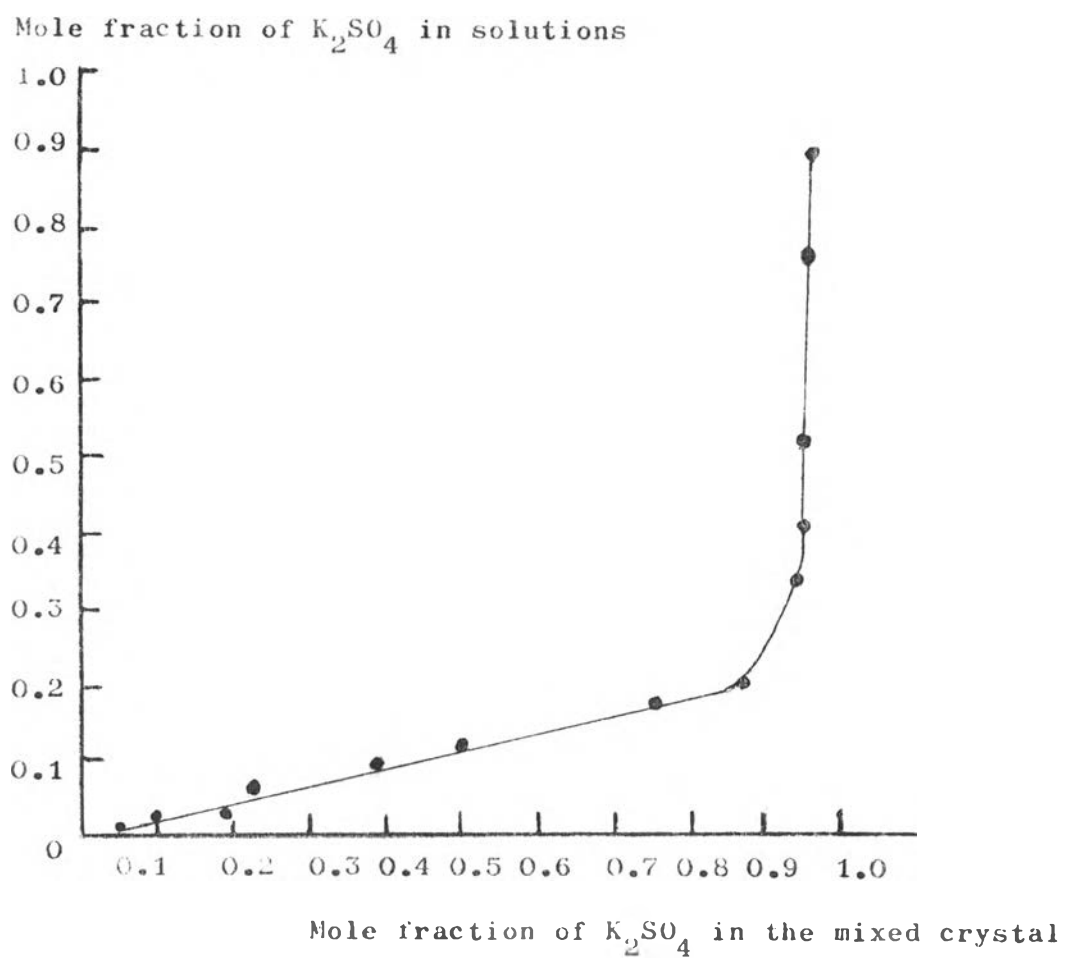


Figure 16. Mole fraction of  $K_2SO_4$  in solution and in the mixed crystals.

Vibrational Spectra of Potassium Chromate and Potassium Sulphate Crystals.

Chromate and sulphate anions have tetrahedral symmetry  $T_d$ . There are nine normal modes of vibration constituting four frequencies of three different symmetry species as shown in Table 13.

Table 13. Spectral activities of ions in point group  $T_d$ .

Mode	Symmetry Species	Activity
$\nu_1$ , stretching	$A_1$	Raman
$\nu_2$ , doubly degenerate deformation	E	Raman
$\nu_3$ , triply degenerate stretching	$T_2$	Raman, infrared
$\nu_4$ , triply degenerate deformation	$T_2$	Raman, infrared

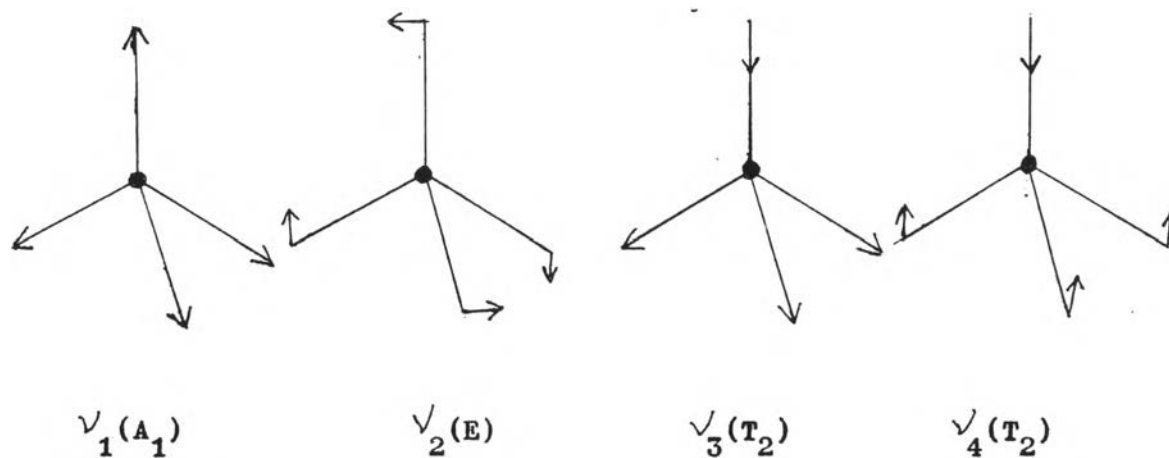


Figure.17 The vibrations of ions in point group  $T_d$  .

The selection rules for free ions having point group  $T_d$  are inadequate to describe the observed infrared and Raman spectra of the crystals as their spectra are very complex. It is also inadequate to interpret these spectra on the basis of site group symmetry for the anions as it cannot describe the effects due to the interactions of a given ion with its neighbour, therefore it is

necessary to use the factor group approximation. The treatment considers the vibrational modes of the crystal as arising from motion of the atoms in the unit cell. The selection rules are derived from the factor group symmetry  $D_{2h}$  which is isomorphic with the space group symmetry  $D_{2h}^{16}$  (Pnma). The factor group approximation allows for the coupling of vibrations between ions.

Both potassium chromate and potassium sulphate have space group symmetry  $D_{2h}^{16}$  (Pnma) with four formula units per unit cell. The site symmetry of both the cations and anions is  $C_s$ . The factor group is  $D_{2h}$ . The molecular point group is  $T_d$ . The correlation between molecular point group ( $T_d$ ), site group ( $C_s$ ) and factor group ( $D_{2h}$ ) was given in Table 14.

Table 14. Correlation diagram between molecular, site and factor groups of potassium chromate, potassium sulphate.

Molecular point group	Site group	Factor group
$T_d$	$C_s$	$D_{2h}$
$A_1$ ( $\checkmark_1$ ) (R)	$A'$ (R,IR)	$A_g + B_{2g} + B_{1u} + B_{3u}$
$E$ ( $\checkmark_2$ ) (R)	$A'$ (R,IR)	$A_g + B_{2g} + B_{1u} + B_{3u}$
	$A''$ (R,IR)	$B_{1g} + B_{3g} + A_u + B_{2u}$
$T_2$ ( $\checkmark_3, \checkmark_4$ ) (R,IR)	$A'$ (R,IR)	$A_g + B_{2g} + B_{1u} + B_{3u}$
	$A'$ (R,IR)	$A_g + B_{2g} + B_{1u} + B_{3u}$
	$A''$ (R,IR)	$B_{1g} + B_{3g} + A_u + B_{2u}$

Note. For  $D_{2h}$  all modes are allowed either in infrared (IR) or Raman (R) with the exception of  $A_u$ .

These correlations were compared with the data in Table 15, 16 which were Raman and infrared frequencies of potassium sulphate and potassium chromate. The Raman and infrared spectra of potassium sulphate were shown in Figures 18, 19 and those of potassium chromate are shown in Figures 20, 21.

Table 15. Vibrational frequencies ( $\text{cm}^{-1}$ ) of potassium sulphate.

Mode	Frequencies ( $\text{cm}^{-1}$ )					Symmetries		
	Raman			Infrared		Molecular point group $T_d$	Site group $C_s$	Factor group $D_{2h}$
	Observed	Reference 18	Reference 19	Observed	Reference 16			
$\nu_1$	983	984	983	983	983	} $A_1$ }	} A }	$A_g$ $B_{2g}$ $B_{3u}$
$\nu_2$	447	445	447			} E }	} A }	$A_g$ $B_{2g}$ $B_{1u}$ $B_{3u}$ $B_{3g}$ $B_{1g}$ $B_{2u}$
	453	456	453	-	448			
				-	448			
	457	455	457					
	-	452	456				} A }	
				-	454			

Table 15. Vibrational frequencies ( $\text{cm}^{-1}$ ) of potassium sulphate.  
(cont.)

Mode	Frequencies ( $\text{cm}^{-1}$ )					Symmetries		
	Raman			Infrared		Mole- cular point $T_d$	Site group $C_s$	Factor group $D_{2h}$
	Observed	Reference 18	Reference 19	Observed	Reference 16			
$\nu_3$	1093	1093	1093			$T_2$	A	$A_g$
	1105	1104	1110.5					$B_{2g}$
				-	1105			$B_{1u}$
				-	1123		$B_{3u}$	
	1110	1110	1109				A	$B_{1g}$
		1104	1104.5					$B_{3g}$
				1108	1108			$B_{2u}$
	1145	1146	1145				A	$A_g$
			1164					$B_{2g}$
				1143	1140			$B_{1u}$
			-	1160	$B_{3u}$			
$\nu_4$	616	614	617			$T_2$	A	$A_g$
		619	619.5					$B_{2g}$
				617	617			$B_{1u}$
				-	618		$B_{3u}$	
		618	622				A	$B_{1g}$
	620	619	620.5					$B_{3g}$
				-	614.4			$B_{2u}$
	628.5	627	627				A	$A_g$
			633.5					$B_{2g}$
			-	623.5	$B_{1u}$			
			-	624.5	$B_{3u}$			

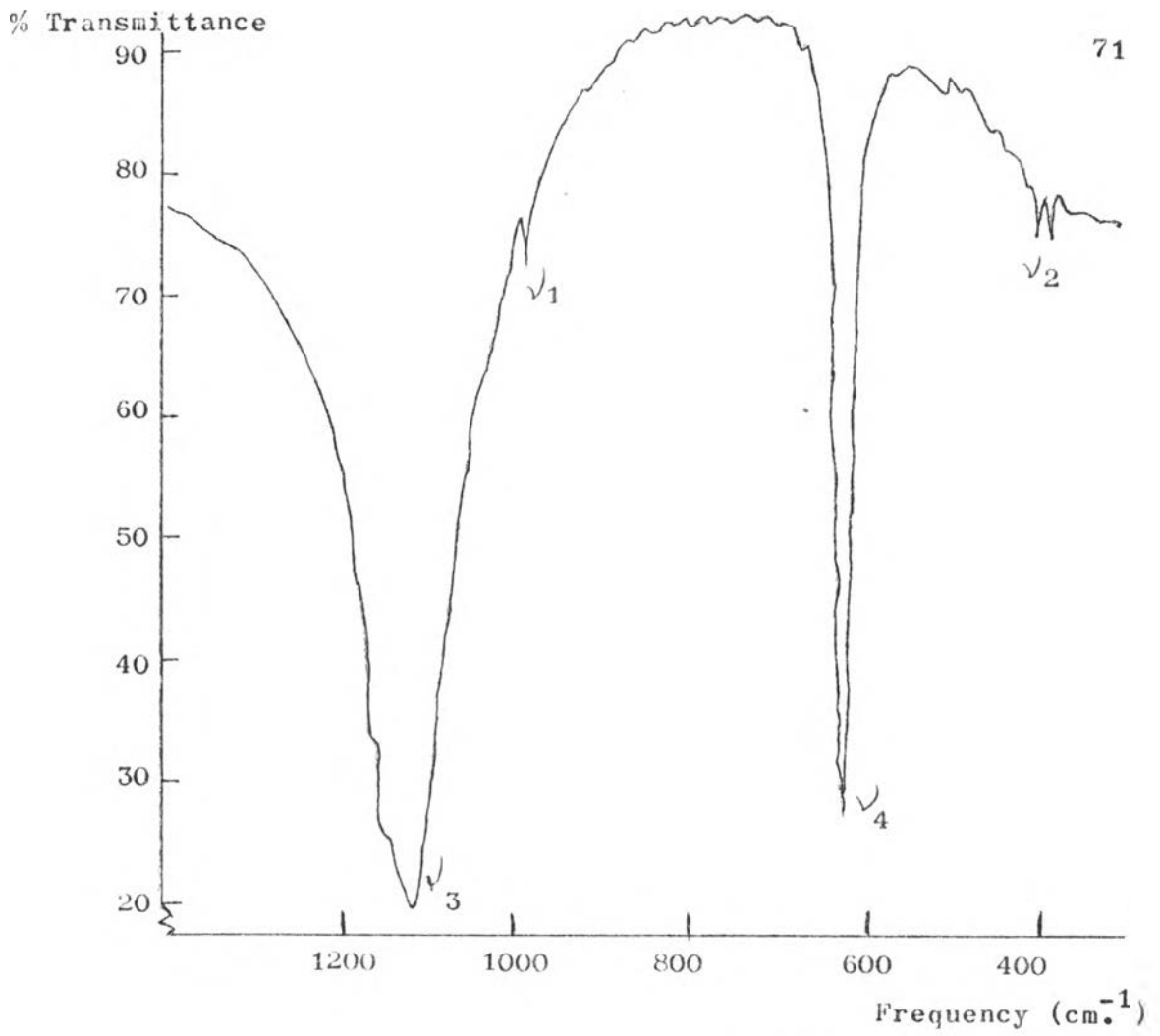


Figure 18. Infrared spectrum of potassium sulphate.

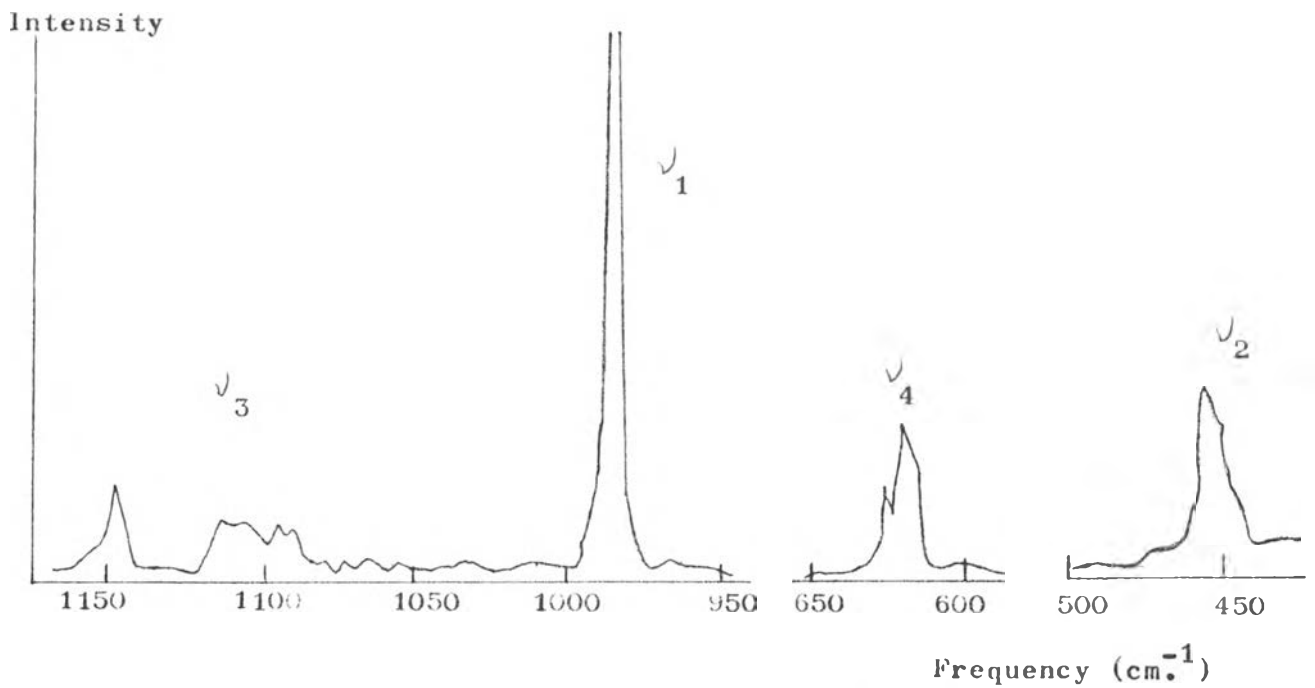


Figure 19. Raman spectrum of potassium sulphate.

Table 16. Vibrational frequencies ( $\text{cm}^{-1}$ ) of potassium chromate.

Mode	Frequencies ( $\text{cm}^{-1}$ )				Symmetries		
	Raman		Infrared		Molecular point group $T_d$	Site group $C_s$	Factor group $D_{2h}$
	Observed	Reference	Observed	Reference			
		30		30			
$\nu_1$	847	851			A <sub>1</sub>	A'	A <sub>g</sub> B <sub>2g</sub> B <sub>3u</sub>
	847	851	851	850			
$\nu_2$	344	345			E	A'	A <sub>g</sub> B <sub>2g</sub> B <sub>1u</sub> B <sub>3u</sub> B <sub>3g</sub> B <sub>1g</sub> B <sub>2u</sub>
	-	350	342	342			
	-	346					
	-	350					
$\nu_3$	862	867			T <sub>2</sub>	A'	A <sub>g</sub> B <sub>2g</sub> B <sub>1u</sub> B <sub>3u</sub> B <sub>1g</sub> B <sub>3g</sub> B <sub>2u</sub> A <sub>g</sub> B <sub>2g</sub> B <sub>1u</sub> B <sub>3u</sub>
		881	-	859			
	872	876					
	-	878	887	883			
	898	903					
	-	918	912	910			
			936			A'	

Table 16. Vibrational frequencies ( $\text{cm}^{-1}$ ) of potassium chromate.  
(cont.)

Mode	Frequencies ( $\text{cm}^{-1}$ )				Symmetries		
	Raman		Infrared		Molecular point group $T_d$	Site group $C_s$	Factor group $D_{2h}$
	Observed	Reference 30	Observed	Reference 30			
$\nu_4$	382	386			}	}	$A_g$
	382	386					$B_{2g}$
							$B_{1u}$
							$B_{3u}$
	-	392					$B_{1g}$
	389	387					$B_{3g}$
			383	382	}	}	$B_{2u}$
	392	396					$A_g$
	392	396					$B_{2g}$
			395	398			$B_{1u}$
						$B_{3u}$	



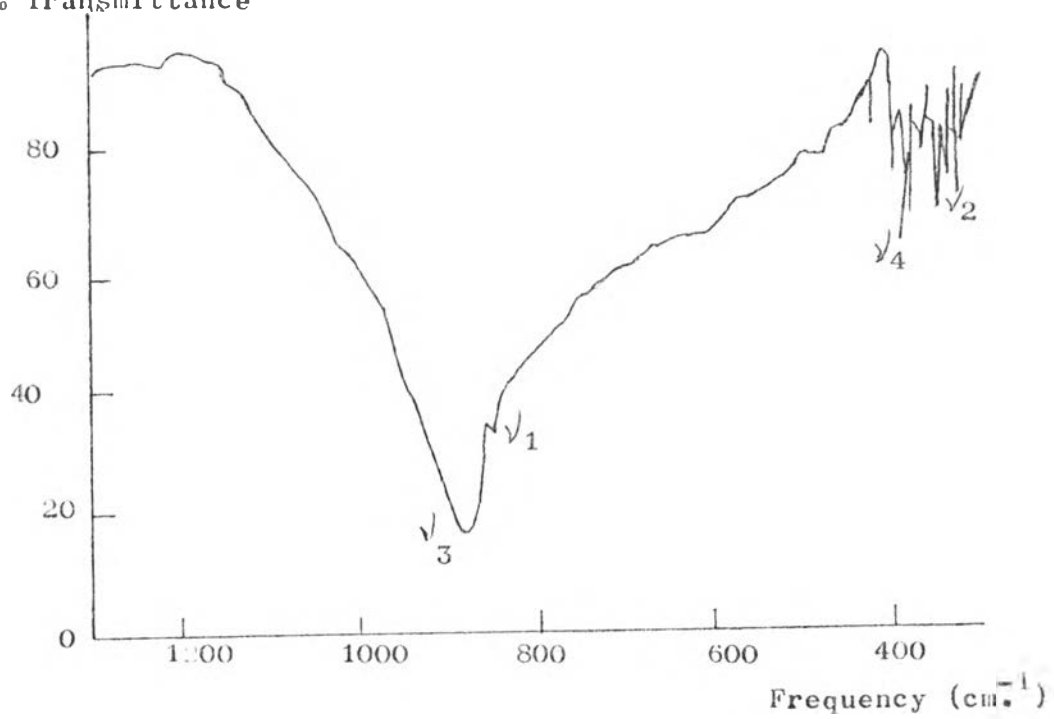


Figure 20. Infrared spectrum of potassium chromate.

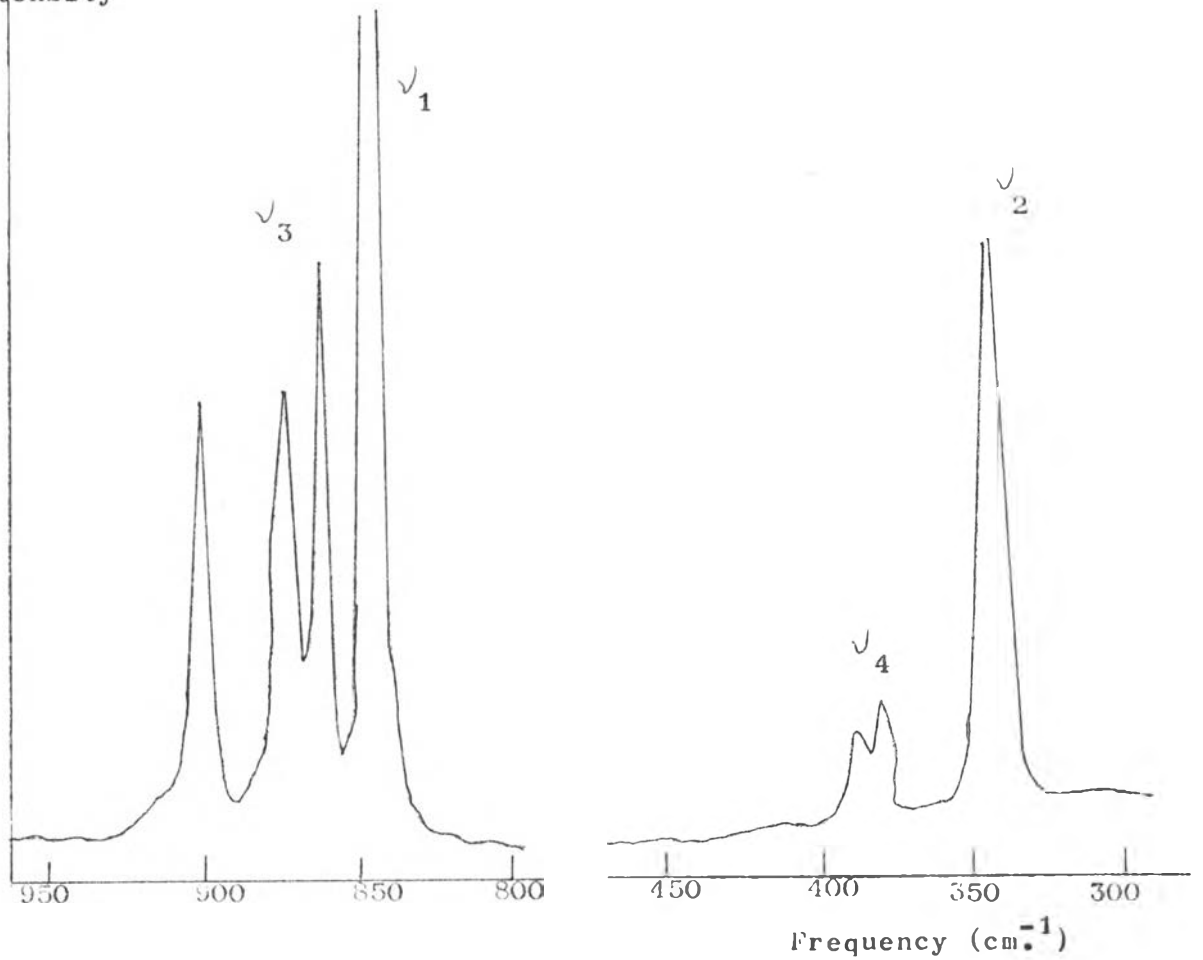


Figure 21. Raman spectrum of potassium chromate.

Vibrational Spectra of Potassium Sulphate.

$\nu_1$  mode.

In the stretching  $\nu_1$  mode, there was no evidence of splitting. Potassium sulphate did not show any vibrational coupling.

In Raman frequency data only one peak was observed at  $983 \text{ cm.}^{-1}$  (agreed with the frequency at  $984, 983 \text{ cm.}^{-1}$  in reference 18 and 19 ).

In the infrared frequency data, this mode also showed only one peak at  $983 \text{ cm.}^{-1}$  (agreed with  $983 \text{ cm.}^{-1}$  in reference 16 ).

$\nu_2$  mode.

The lowest frequency mode was the doubly degenerate deformation  $\nu_2$ . This degeneracy was relieved in the  $C_s$  site group symmetry and in the factor group symmetry  $D_{2h}$ . Site splitting gave one component symmetric ( $A'$ ) and one antisymmetric ( $A''$ ) with respect to reflection in the mirror plane.  $A'$  gave  $A_g + B_{2g} + B_{1u} + B_{3u}$  factor group components.  $A''$  gave  $B_{1g} + B_{3g} + B_{2u}$  factor group components.

The observed Raman frequency data of potassium sulphate were rewritten in Table 17 showing the separation of frequencies and the mean value,  $\bar{X}$  (or the center of gravity) of each set of frequencies.

Table 17 Raman frequency data in  $\nu_2$  mode of potassium sulphate.

Symmetry		Frequencies ( $\text{cm}^{-1}$ )														
$C_s$	$D_{2h}$	Observed	$\bar{X}$	$\Delta\nu_s$	$\Delta\nu_T$	$\Delta\nu_f$	Reference 18	$\bar{X}$	$\Delta\nu_s$	$\Delta\nu_T$	$\Delta\nu_f$	Reference 19	$\bar{X}$	$\Delta\nu_s$	$\Delta\nu_T$	$\Delta\nu_f$
A	A <sub>g</sub>	447	450	7	10	3	445	450	3.5	106.5		447	450			
	B <sub>2g</sub>	453					456					453				
A	B <sub>2g</sub>	457	457				455	453.5				457	456.5			
	B <sub>1g</sub>					452		456								

Mean value ( $\bar{X}$ ) was taken by averaging the frequencies of one set, such as,  $\bar{X} = \frac{447+453}{2} = 450$ .

Site group splitting ( $\Delta\nu_s$ ) was taken from the difference between the mean values of frequency sets (A', A''), such as,  $\Delta\nu_s = 457-450 = 7$ .

An overall spread or the total frequency difference ( $\Delta\nu_T$ ) was taken from the difference between the lowest frequency of one set and the highest frequency of the other set, such as,  $\Delta\nu_T = 457-447 = 10$ .

Factor group splitting ( $\Delta\nu_f$ ) was taken from the difference between an overall spread and site group splitting.  $\Delta\nu_f = \Delta\nu_T - \Delta\nu_s$  such as,  $\Delta\nu_f = 10-7 = 3$ .

So the site group and factor group splitting in the  $\nu_2$  mode were shown in Table 18.

Table 18 The site group splitting ( $\Delta\nu_s$ ) and factor group splitting ( $\Delta\nu_f$ ) in Raman  $\nu_2$  mode of potassium sulphate.

	Observed	Reference 18	Reference 19
$\Delta\nu_s, A' - A''$	7	3.5	6.5
$\Delta\nu_f, A' - A''$	3	6.5	3.5

It was seen that site group and factor group splittings were comparable

In the infrared frequency data,  $\nu_2$  mode was not observed though it was reported in reference 16 .

$\nu_3$  mode.

The triply degenerate stretching mode  $\nu_3$ , showed a clear site splitting which gave 2  $A'$  and  $A''$  components.  $A'$  gave  $A_g + B_{2g} + B_{1u} + B_{3u}$  factor group components.  $A''$  gave  $B_{1g} + B_{3g} + B_{2u}$  factor group components.

In Raman data there was factor group splitting in  $A'$  but not in  $A''$ .

Table 19 Raman frequency data in  $\nu_3$  mode of potassium sulphate.

Symmetry		Frequencies (cm <sup>-1</sup> )															
		C <sub>S</sub> D <sub>2h</sub>	Obs.	$\bar{X}$	$\Delta\nu_s$	$\Delta\nu_T$	$\Delta\nu_f$	Ref.	$\bar{X}$	$\Delta\nu_s$	$\Delta\nu_T$	$\Delta\nu_f$	Ref.	$\bar{X}$	$\Delta\nu_s$	$\Delta\nu_T$	$\Delta\nu_f$
							18					19					
A	A <sub>g</sub>	1093		1099			1093		1098.5			1093		1101.7			
	B <sub>2g</sub>	1105					1104					1110.5					
					11	17	6							5		16	11
A	B <sub>1g</sub>	1110		1110			1110		1107			1109		1106.7			
	B <sub>3g</sub>	-					1104					1104.5					
					35	35	0			39	42	3			47.8		
A	A <sub>g</sub>	1145		1145			1146		1146			1145		1154.5		59.5	11.7
	B <sub>2g</sub>	-					-					1164					

Table 20. The site group splitting ( $\Delta\nu_s$ ) and factor group splitting ( $\Delta\nu_f$ ) in Raman  $\nu_3$  mode of potassium sulphate.

		Observed	Reference	Reference
			18	19
$\Delta\nu_s$ (cm <sup>-1</sup> )	A-A	11	8.5	5
	A-A	35	39	47.8
$\Delta\nu_f$ (cm <sup>-1</sup> )	A-A	6	8.5	11
	A-A	-	3	11.7

In the infrared data, only two peaks were observed at 1108, 1143  $\text{cm}^{-1}$  and there was no factor group splitting. The separation of frequencies and the mean value of each set of frequencies were shown in Table 21.

Table 21. Infrared frequency data in  $\sqrt{3}$  mode of potassium sulphate

Symmetry		Frequencies ( $\text{cm}^{-1}$ )									
$C_s$	$D_{2h}$	Observed	$\bar{X}$	$\Delta\nu_s$	$\Delta\nu_T$	$\Delta\nu_f$	Reference	$\bar{X}$	$\Delta\nu_s$	$\Delta\nu_T$	$\Delta\nu_f$
							16				
/	A } $B_{1u}$	-	-				1105	1114			
		-					1123				
				-	-	-			6	3	3
//	A } $B_{2u}$	1108	1108				1108	1108			
				35	35	0			42	52	10
/	A } $B_{1u}$	1143	1143				1140	1150			
		-					1160				

Table 22 The site group and factor group splitting in the infrared  $\sqrt{3}$  mode of potassium sulphate.

	Observed	Reference
		16
$\Delta\nu_s$ , $\overset{1}{A}-\overset{1}{A}$	-	6
( $\text{cm}^{-1}$ ) $\overset{1}{A}-\overset{1}{A}$	35	42
$\Delta\nu_f$ , $\overset{1}{A}-\overset{1}{A}$	-	3
( $\text{cm}^{-1}$ ) $\overset{1}{A}-\overset{1}{A}$	-	10

$\nu_4$  mode.

In the triply degenerate deformation mode  $\nu_4$ , site splitting gave  $2A'$  and  $A''$  components.  $A'$  gave  $A_g + B_{2g} + B_{1u} + B_{3u}$  factor group components.  $A''$  gave  $B_{1g} + B_{3g} + B_{2u}$  factor group components.

The observed Raman data showed site group splitting but no factor group splitting, as shown in Table 23.

Table 23. Raman frequency data in  $\nu_4$  mode of potassium sulphate

Symmetry		Frequencies (cm <sup>-1</sup> )														
$C_s$	$D_{2h}$	Obs.	$\bar{X}$	$\Delta\nu_s$	$\Delta\nu_T$	$\Delta\nu_f$	Ref.	$\bar{X}$	$\Delta\nu_s$	$\Delta\nu_T$	$\Delta\nu_f$	Ref.	$\bar{X}$	$\Delta\nu_s$	$\Delta\nu_T$	$\Delta\nu_f$
							18					19				
A	$A_g$	616	616	4	4	0	614	616.5	2	5	3	617	618.3	3	5	2
	$B_{2g}$	-					619					619.5				
A	$B_{1g}$	620	620	8.5	8.5	0	618	618.5	8.5	8	0.5	622	621.3	9	13	4
	$B_{3g}$	-					619					620.5				
A	$A_g$	628.5	628.5	-	-	-	627	627	-	-	-	627	630.3	-	-	-
	$B_{2g}$	-					-					633.5				

Table 24. The site group and factor group splittings in Raman  $\nu_4$  mode of potassium sulphate.

	Observed	Reference	
		18	19
$\Delta\nu_s$ , $A-A$ (cm <sup>-1</sup> )	4	2	3
$\Delta\nu_s$ , $A-A$ (cm <sup>-1</sup> )	8.5	8.5	9
$\Delta\nu_f$ , $A-A$ (cm <sup>-1</sup> )	-	3	2
$\Delta\nu_f$ , $A-A$ (cm <sup>-1</sup> )	-	0.5	4

In the infrared data of  $\nu_4$  mode, only one peak at  $617 \text{ cm}^{-1}$  was observed though there were site group and factor group splittings in reference 16.

### Vibrational Spectra of Potassium Chromate

#### $\nu_1$ mode.

In the stretching  $\nu_1$  mode, there was no evidence of splitting. Potassium chromate did not show any vibrational coupling.

In Raman data only one peak was observed at  $847 \text{ cm}^{-1}$  (agreed with  $851 \text{ cm}^{-1}$  in reference 30).

In the infrared data, this mode also showed only one peak at  $851 \text{ cm}^{-1}$  (agreed with  $850 \text{ cm}^{-1}$  in reference 30).

#### $\nu_2$ mode.

The lowest frequency mode is the doubly degenerate deformation  $\nu_2$ . This degeneracy should be relieved in the site group symmetry  $C_2$  and in the factor group symmetry  $D_{2h}$  but the observed Raman data showed no splitting. There was only one peak at  $344 \text{ cm}^{-1}$  (in reference 30 there was a splitting in this mode).

In the infrared data one peak at  $342 \text{ cm}^{-1}$  was observed (agreed with  $342 \text{ cm}^{-1}$  in reference 30).

#### $\nu_3$ mode.

The triply degenerate stretching mode  $\nu_3$ , showed site splitting giving  $2A'$  and  $A''$  components both in Raman and infrared spectra. There was no factor group splitting observed. The site group and factor group splittings of potassium chromate were found by the same procedure described in potassium sulphate so only the results were shown.

Table 25 The site group and factor group splittings in Raman  $\nu_3$  mode of potassium chromate.

	Observed	Reference
		30
$\Delta\nu_s$ , $A-A''$	10	3
$A-A'$	26	33.5
$\Delta\nu_f$ , $A-A''$	-	8
$A-A'$	-	6.5



Table 26 The site group and factor group splittings in the infrared  $\nu_3$  mode of potassium chromate.

	Observed	Reference
		30
$\Delta\nu_s$ , $A-A''$	-	24
$A-A'$	25	40
$\Delta\nu_f$ , $A-A''$	-	-
$A-A'$	-	13

$\nu_4$  mode.

The triply degenerate deformation mode  $\nu_4$ , showed site group and factor group splittings in Raman spectra.

Table 27 The site group and factor group splittings in Raman  $\nu_4$  mode of potassium chromate.

	Observed	Reference
		30
$\Delta\nu_s$ , $A-A''$	7	3.5
$A-A'$	3	6.5
$\Delta\nu_f$ , $A-A''$	-	2.5
$A-A'$	-	2.5



In the infrared data, two peaks were observed at 383, 395  $\text{cm}^{-1}$  (agreed with 382, 398  $\text{cm}^{-1}$  in reference 30 ).

In a recent reinterpretation of the internal vibrational spectra of phase 1 of ammonium sulphate ( 34 ) it was demonstrated that the arrangement of the ions within the crystal lattice had a major influence on the observed spectra. Specifically, the sulphate anions were packed such that all anions had a local threefold axis parallel to the crystallographic c-axis. The splitting of the  $T_2$  modes of sulphate anion into two components ( $A+E$ ) with a 1:2 intensity ratio was explained by  $C_{3v}$  point group symmetry.

Both potassium sulphate and potassium chromate are isomorphous with ammonium sulphate and are expected to have the same effects in their vibrational spectra. A study of their structures showed that the anions all have local  $C_3$  axes lying in a crystallographic mirror plane approximately parallel to the  $\pi$ -axis (Figure 22 ). Although this threefold axis is only local, the arrangement of surrounding anions and cations is such that local x, y degeneracy is approximately preserved. It will be demonstrated that the local  $C_3$  axis exerts a major spectral influence.

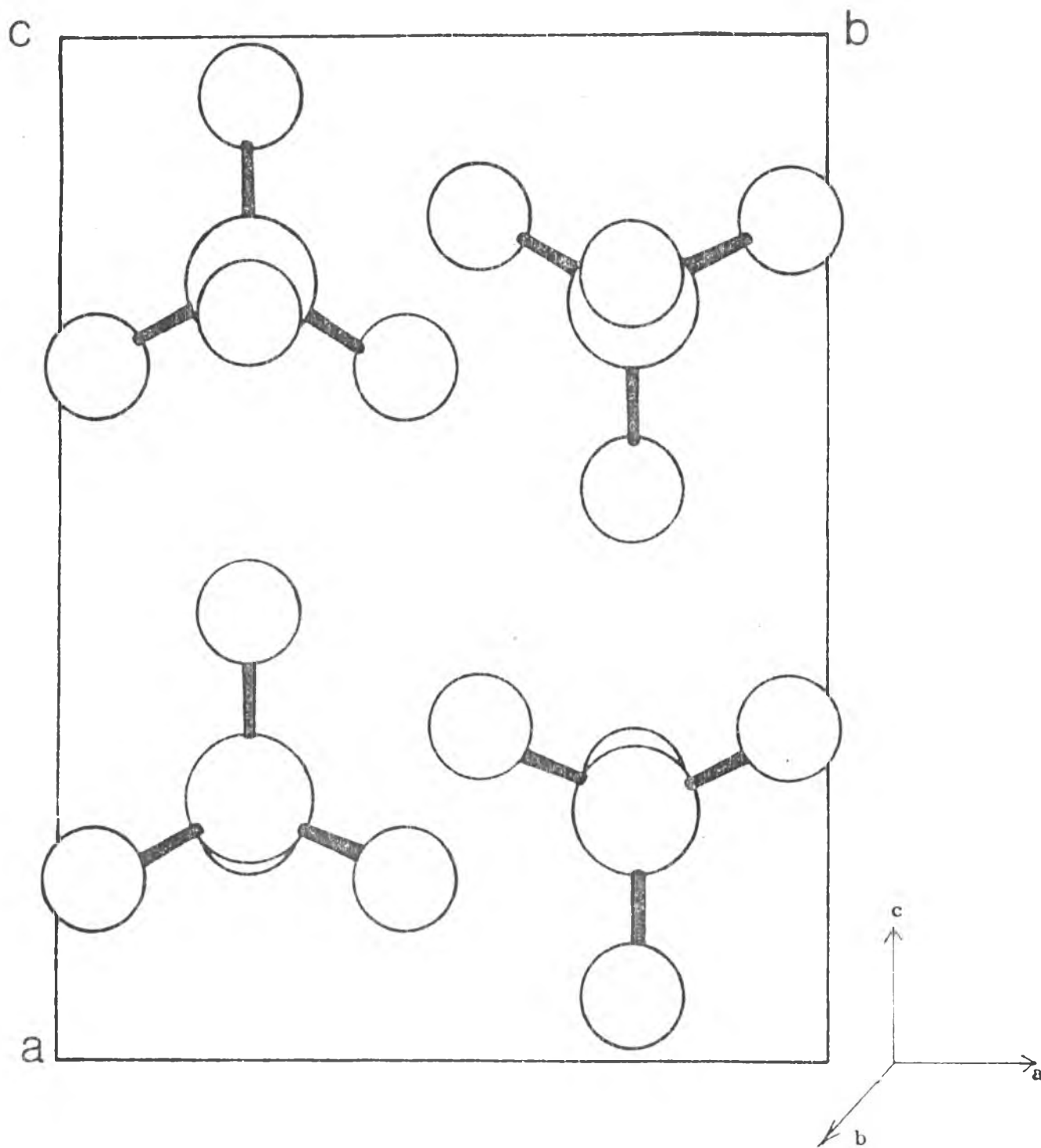


Figure 22 . The crystal structure of potassium sulphate viewed down the c-axis. Just the sulphate ions in one unit cell were shown. (The crystal structure of potassium chromate was the same).

The Correlation Tables for the Descent of Symmetry

The active modes in the molecules when the symmetry of crystal is reduced are predicted by the correlation tables showing how the representations are reduced to the simpler ones.

Table 28. The correlation of irreducible representations between  $T_d$  and  $C_{3v}$  point group symmetries.

$T_d$	$C_{3v}$
$A_1$	$A_1$
E	E
$T_2$	$A_1 + E$

According to the character tables for  $C_{3v}$  and  $T_d$ ,  $C_3$  is the common symmetry element. The comparison between the character of each representation under  $C_3$  of  $C_{3v}$  to  $T_d$  showed that  $A_1$  of  $C_{3v}$  corresponds to  $A_1$  of  $T_d$ , E of  $C_{3v}$  corresponds to E of  $T_d$  and  $A_1 + E$  of  $C_{3v}$  correspond to  $T_2$  of  $T_d$ .

Table 29. The character table for  $T_d$ .

$T_d$ (h=24)	E	$8C_3$	$3C_2$	$6S_4$	$6\sigma_d$	
$A_1$	1	1	1	1	1	$x^2 + y^2 + z^2$
$A_2$	1	1	1	-1	-1	
E	2	-1	2	0	0	$(x^2 - y^2, 2z^2 - x^2 - y^2)$
$T_1$	3	0	-1	1	-1	$(R_x, R_y, R_z)$
$T_2$	3	0	-1	-1	1	$(xy, xz, yz)$

Table 30. The character table for  $C_{3v}$ 

$C_{3v} (h=6)$	E	$2 C_3(z)$	$3 C_2$		
$A_1$	1	1	1	z	$x^2 + y^2, z^2$
$A_2$	1	1	-1	$R_z$	
E	2	-1	0	$(x, y) (R_x, R_y)$	$(x^2 - y^2, xy) (xz, yz)$

The correlation between  $C_{3v}$  and  $D_{2h}$  was shown in Table 31.

Table 31. The correlation table between  $C_{3v}$  and  $D_{2h}$ .

$C_{3v}$	$D_{2h}$
$A_1$	$A_g + B_{2g} + B_{1u} + B_{3u}$
E	$A_g + B_{1g} + B_{2g} + B_{3g} + A_u + B_u + B_{2u} + B_{3u}$

This correlation was found by the same procedure as described above. According to the character tables of  $C_{3v}$  and  $D_{2h}$ ,  $C_v$  is the common symmetry element ( $C_v$  of  $C_{3v}$  and  $C_{xz}$  of  $D_{2h}$ ). The comparison between the character of each representation under  $C_v$  of  $C_{3v}$  to  $C_{xz}$  of  $D_{2h}$  showed the results as in Table 31.

Table 32. The character table for  $D_{2h}$ 

$D_{2h} (h=8)$	E	$C_2(z)$	$C_2(y)$	$C_2(x)$	i	$\sigma(xy)$	$\sigma(xz)$	$\sigma(yz)$		
$A_g$	1	1	1	1	1	1	1	1		$x^2, y^2, z^2$
$B_{1g}$	1	1	-1	-1	1	1	-1	-1	$R_z$	xy
$B_{2g}$	1	-1	1	-1	1	-1	1	-1	$R_y$	xz
$B_{3g}$	1	-1	-1	1	1	-1	-1	1	$R_x$	yz
$A_u$	1	1	1	1	-1	-1	-1	-1		
$B_{1u}$	1	1	-1	-1	-1	-1	1	1	z	
$B_{2u}$	1	-1	1	-1	-1	1	-1	1	y	
$B_{3u}$	1	-1	-1	1	-1	1	1	-1	x	

The correlation between molecular point group  $T_d$ , local  $C_{3v}$  and factor group  $D_{2h}$  was given in Table 33.

Table 33 The correlation diagram between molecular point group  $T_d$ , local  $C_{3v}$  and factor group  $D_{2h}$

Molecular point group $T_d$	Local $C_{3v}$	Factor group $D_{2h}$
$A_1 (\checkmark_1)$ (R)	$A_1$ (R, IR)	$A_g + B_{2g} + B_{1u} + B_{3u}$
$E (\checkmark_2)$ (R)	$E$ (R, IR)	$A_g + B_{1g} + B_{2g} + B_{3g} + A_u + B_u + B_{2u} + B_{3u}$
$T_2 (\checkmark_3, \checkmark_4)$ (R, IR)	$A_1$ (R, IR)	$A_g + B_{2g} + B_{1u} + B_{3u}$
	$E$ (R, IR)	$A_g + B_{1g} + B_{2g} + B_{3g} + A_u + B_u + B_{2u} + B_{3u}$

Note. For  $D_{2h}$  all modes are allowed either in infrared (IR) or Raman (R) with the exception of  $A_u$ .

These correlations were compared with the data of Raman and infrared frequencies of potassium sulphate and potassium chromate in Table 34, 35.

Table 34. Vibrational frequencies ( $\text{cm}^{-1}$ ) of potassium sulphate.

Mode	Frequencies ( $\text{cm}^{-1}$ )					Symmetries		
	Raman			Infrared		Molecular point group $T_d$	Local $C_{3v}$	Factor group $D_{2h}$
	Observed	Reference 18	Reference 19	Observed	Reference 16			
$\nu_1$	983	984	983	983	983	$A_1$	$A_1$	$A_g$ $B_{2g}$ $B_{3u}$
$\nu_2$	447 453 457 -	445 456 455 452	447 453 457 456	- - -	448 448 454	$E$	$E$	$A_g$ $B_{2g}$ $B_{1u}$ $B_{3u}$ $B_{3g}$ $B_{1g}$ $B_{2u}$

Table 34 Vibrational frequencies ( $\text{cm}^{-1}$ ) of potassium sulphate.  
(cont.)

Mode	Frequencies ( $\text{cm}^{-1}$ )					Symmetries		
	Raman			Infrared		Mole- cular point $T_d$	Local $C_{3v}$	Factor group $D_{2h}$
	Observed	Reference 18	Reference 19	Observed	Reference 16			
$\sqrt{3}$	1093	1093	1093			$T_2$	E	$A_g$
	1105	1104	1110.5					$B_{2g}$
				-	1105			$B_{1u}$
				-	1123			$B_{3u}$
	1110	1110	1109					$B_{1g}$
	-	1104	1104.5					$B_{3g}$
				1108	1108			$B_{2u}$
	1145	1146	1145					$A_g$
	-	-	1164					$B_{2g}$
			1143	1140	$A_1$	$B_{1u}$		
			-	1160		$B_{3u}$		
$\sqrt{4}$	616	614	617			$T_2$	E	$A_g$
	-	619	619.5					$B_{2g}$
				617	617			$B_{1u}$
				-	618			$B_{3u}$
	-	618	622					$B_{1g}$
	620	619	620.5					$B_{3g}$
				-	614.4			$B_{2u}$
	628.5	627	627					$A_g$
	-	-	633.5					$A_1$
			-	623.5	$B_{1u}$			
			-	624.5	$B_{3u}$			

Table 35. Vibrational frequencies ( $\text{cm}^{-1}$ ) of potassium chromate.

Mode	Frequencies ( $\text{cm}^{-1}$ )				Symmetries		
	Raman		Infrared		Molecular point group $T_d$	Local $C_{3v}$	Factor group $D_{2h}$
	Observed	Reference	Observed	Reference			
$\nu_1$	847	851			} $A_1$ }	} $A_1$ }	$A_g$ $B_{2g}$ $B_{3u}$
	847	851	851	850			
$\nu_2$	344	345			} E }	} E }	$A_g$ $B_{2g}$ $B_{1u}$ $B_{3u}$ $B_{3g}$ $B_{1g}$ $B_{2u}$
	-	350					
			342	342			
	-	346					
	-	350					
$\nu_3$	862	867			} $T_2$ }	} E }	$A_g$ $B_{2g}$ $B_{1u}$ $B_{3u}$ $B_{1g}$ $B_{3g}$ $B_{2u}$
		881					
			-	859			
	872	876					
	-	878					
			887	883			
	898	903					
	-	918					
		912	910				
		-	936				
					} $A_1$ }	$A_g$ $B_{2g}$ $B_{1u}$ $B_{3u}$	



Table 35. Vibrational frequencies ( $\text{cm}^{-1}$ ) of potassium chromate.  
(cont.)

Mode	Frequencies ( $\text{cm}^{-1}$ )				Symmetries		
	Raman		Infrared		Molecular point group $T_d$	Local $C_{3v}$	Factor group $D_{2h}$
	Observed	Reference 30	Observed	Reference 30			
$\nu_4$	382	386			} $T_2$ }	} E }	$A_g$
	382	386					$B_{2g}$
							$B_{1u}$
							$B_{3u}$
	-	392					$B_{1g}$
	389	387	383	382			$B_{3g}$
							$B_{2u}$
	392	396			} $A_1$ }	$A_g$	
	392	396				$B_{2g}$	
			395	398		$B_{1u}$	
						$B_{3u}$	

Raman spectrum of potassium sulphate in the triply degenerate  $\nu_3$  and  $\nu_4$  regions were shown in Figure 23.

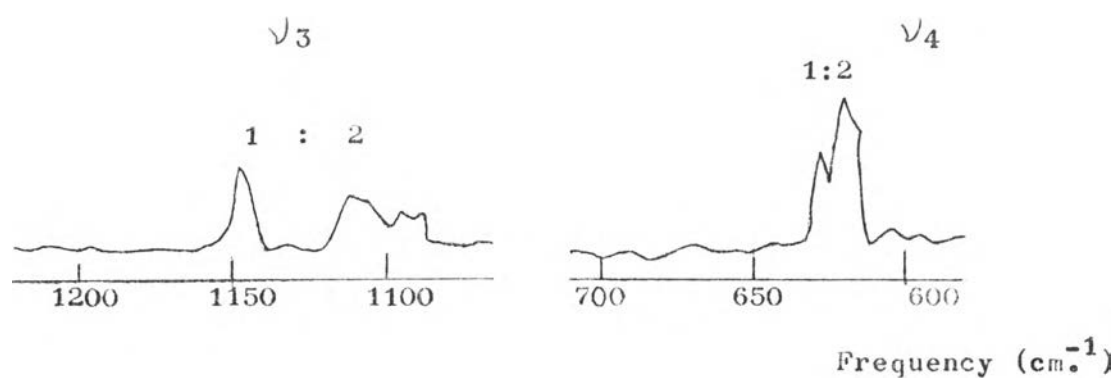


Figure 23. The Raman spectrum of potassium sulphate in the  $\nu_3$  and  $\nu_4$  regions.

$T_2$  (in  $T_d$ ) modes of the sulphate ion exhibited a  $C_{3v}$ -type of spectral behaviour:  $T_2 \longrightarrow A_1 + E$  components with 1:2 intensity ratio. There was an explanation for this behaviour as could be seen in Figure 24.

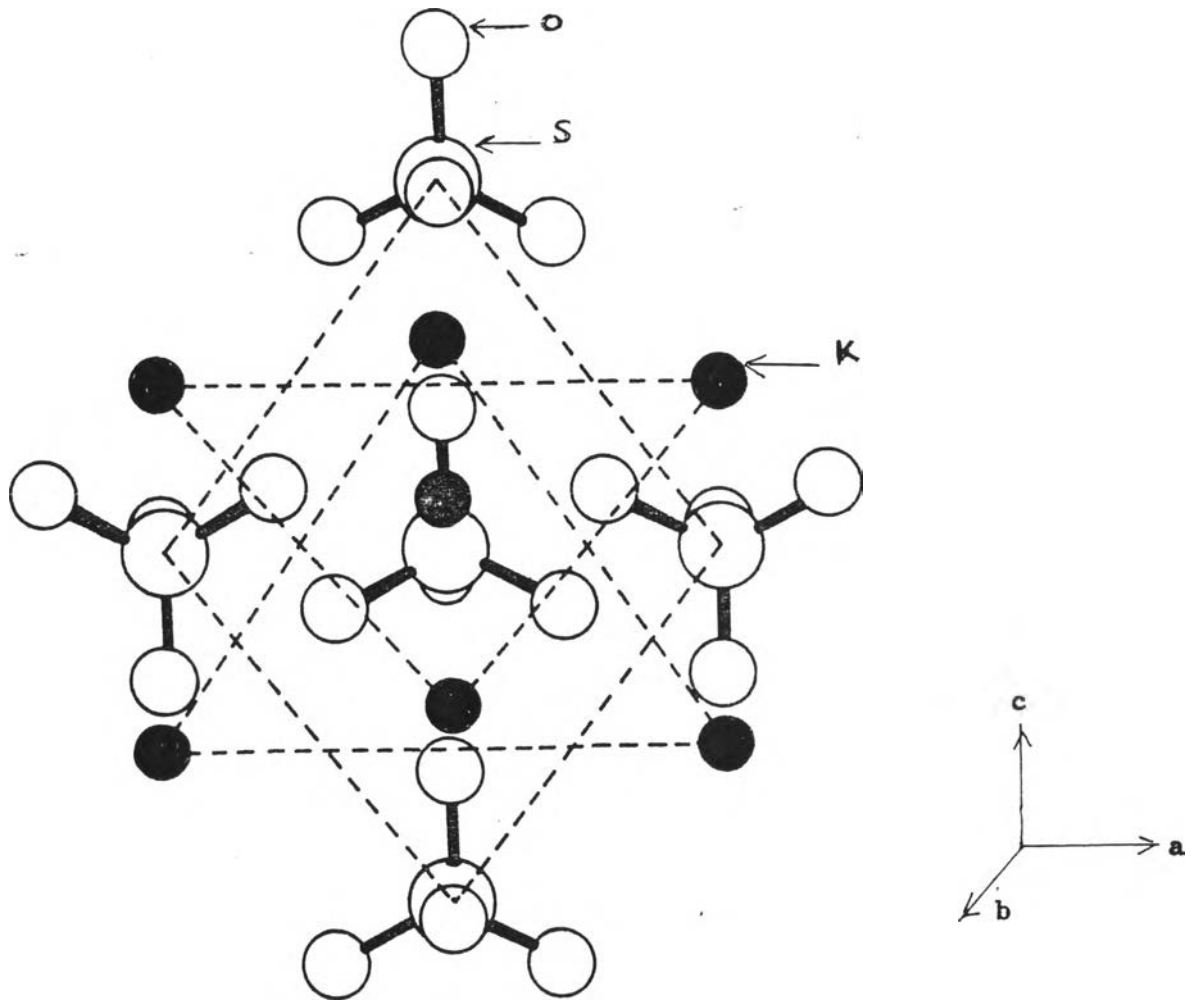


Figure 24. The crystal structure of potassium sulphate viewed down the c-axis, showing the potassium and sulphate groups surrounding the sulphate group highlighted in Figure 22.

Figure 24. gave a view of the potassium sulphate down the c-axis. Each sulphate ion has a threefold axis almost parallel to c-axis. There are potassium ions approximately along this local threefold axis and other surrounding potassium ions lie approximately at the corners of two opposed equilateral triangles. Surrounding sulphate ions lie at the corners of a distorted square. It was seen that for each sulphate ion there is an axis approximately

parallel to the crystallographic c-axis and the arrangement of surrounding groups is such that the local x,y degeneracy is maintained. Thus, the spectral behaviour is explained by  $C_{3v}$  point group symmetry.

Raman spectrum of potassium chromate in the triply degenerate  $\nu_3$  and  $\nu_4$  regions were shown in Figure 25.  $T_2$  (in  $T_d$ ) modes of the chromate ion also exhibited a  $C_{3v}$ -type spectral behaviour:  $T_2 \longrightarrow A_1 + E$  as in the potassium sulphate.

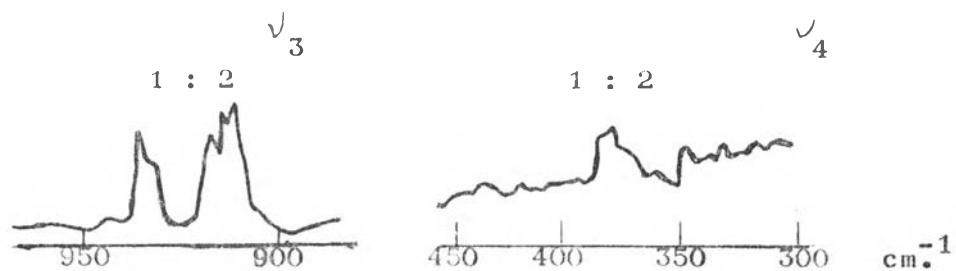
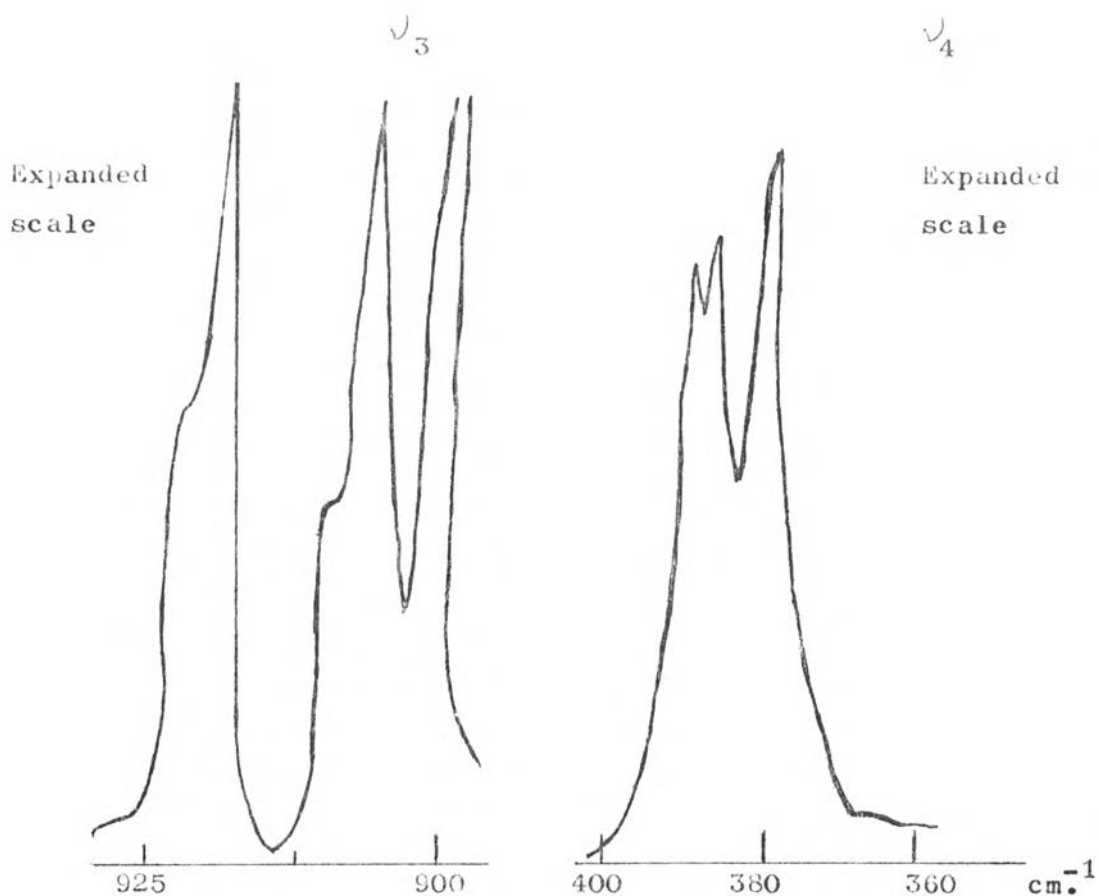


Figure 25. Raman spectrum of potassium chromate in  $\nu_3, \nu_4$  regions.



The above discussion of the vibrational spectra of potassium chromate and potassium sulphate left an uncertainty about some aspects. It was commonly concluded that the site group effect was comparable in magnitude to the factor group effect. There might be a parallel between static (site group) and dynamic (factor group) effects and it was desirable to investigate them separately. This separability could be done by a study of mixed crystals. Potassium chromate and potassium sulphate were isomorphous and they could form mixed crystals so a series of mixed crystals potassium chromate/potassium sulphate over the entire relative concentration range was studied.

#### Vibrational Spectra of Mixed Crystals

The frequencies of potassium sulphate and potassium chromate were well separated that each vibrational unit would couple only with its own kind in the mixed crystals. In the low concentration limit of one component (guest ion) in the mixed crystals, the guest ion was matrix isolated, therefore its vibrational unit would be vibrationally uncoupled and sensitive only to site group effects. So it enabled a distinction between site group and factor group effects. There was a reason to object that the site group effects on sulphate ion in a host of potassium chromate lattice would differ from sulphate ion in its own lattice, although the lattices of potassium chromate and potassium sulphate were isomorphous. In the event, it seemed that this objection was rather weak, because the data led to an interpretation which was almost independent of lattice.

The addition of a guest ion in the formation of a mixed crystal destroyed the translational symmetry of the lattice so that the symmetry designations of the vibrational modes appropriate to the pure crystal were no longer valid. They were retained here only as an aid in labeling the origin of the mixed crystal modes.

### 1. Infrared Spectra of Mixed Crystals

The infrared spectra of the mixed crystals in various concentration compared with pure potassium chromate and pure potassium sulphate were shown in Figure 26 . The frequency data of the mixed crystals were reported in Table 36 . The infrared spectra of the mixtures in various concentration were also shown in Figure 27.

The infrared spectra of the mixed crystals differed from the spectra of the two pure crystals with respect to the frequencies and relative intensities of the modes. Mechanically mixing of the two pure crystals gave infrared spectrum which closely resembled a simple superposition of their components.

% Transmittance

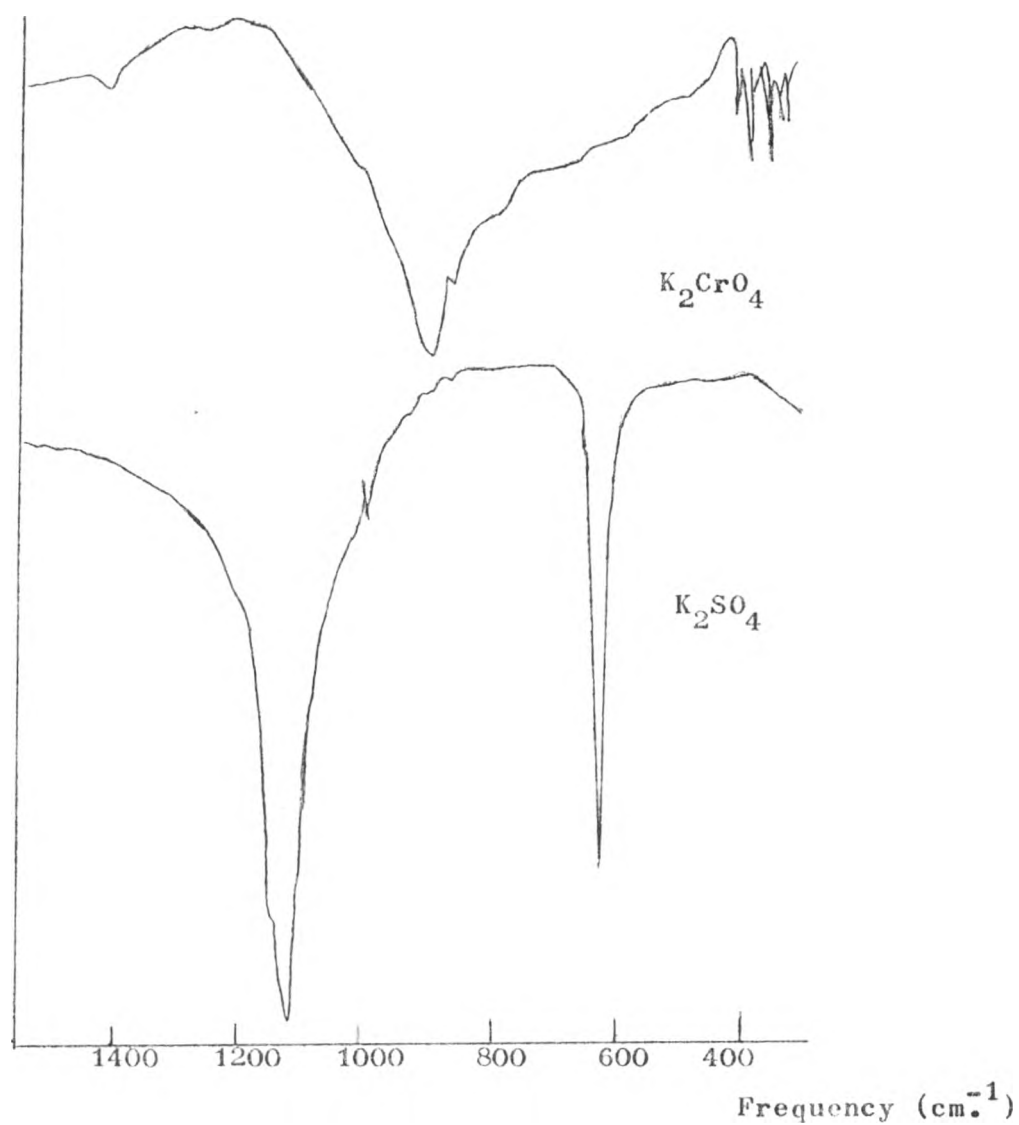


Figure 26. The infrared spectra of potassium chromate, potassium sulphate (compared with the mixed crystals).

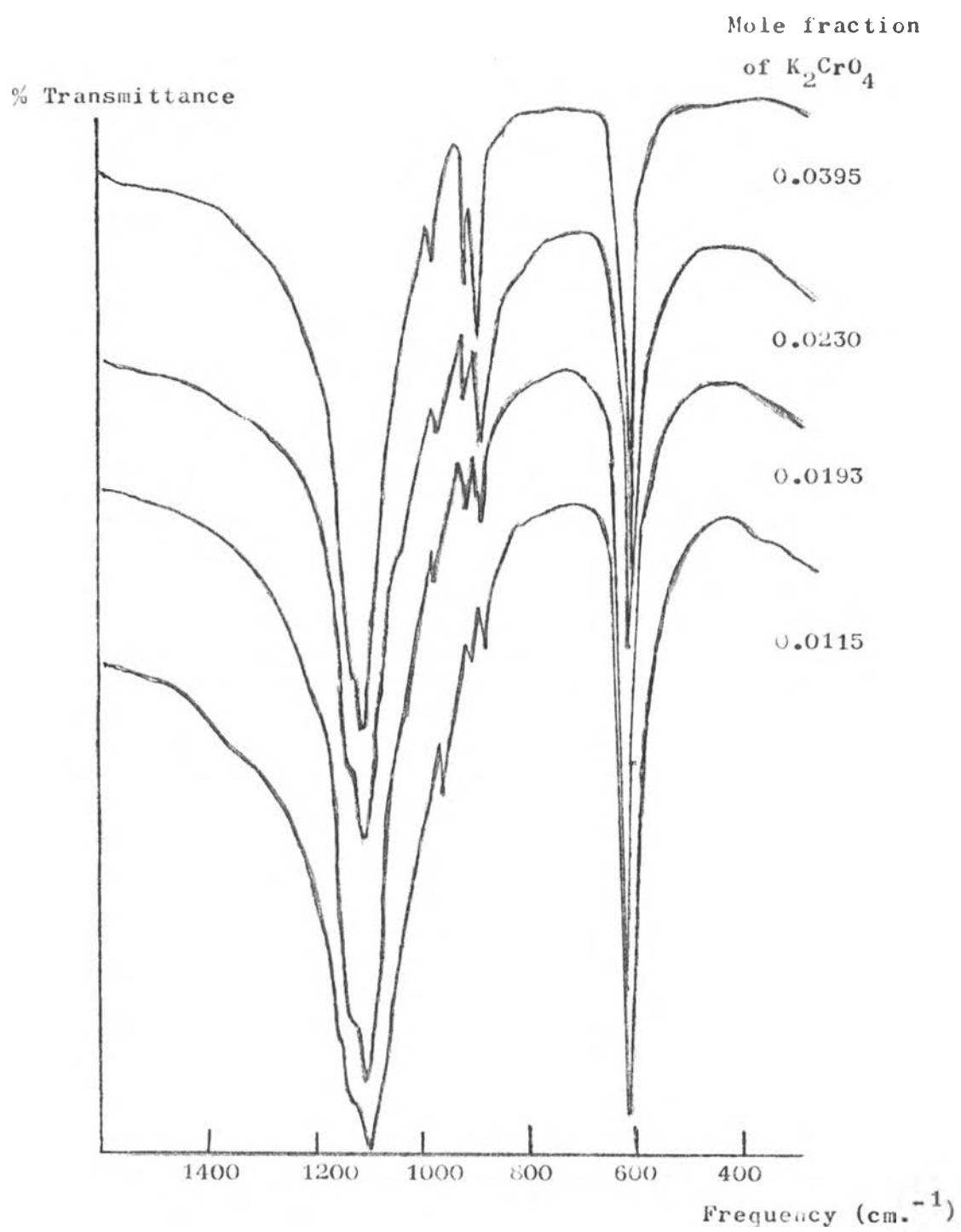


Figure 26a. The infrared spectra of the mixed crystals.

(cont.)



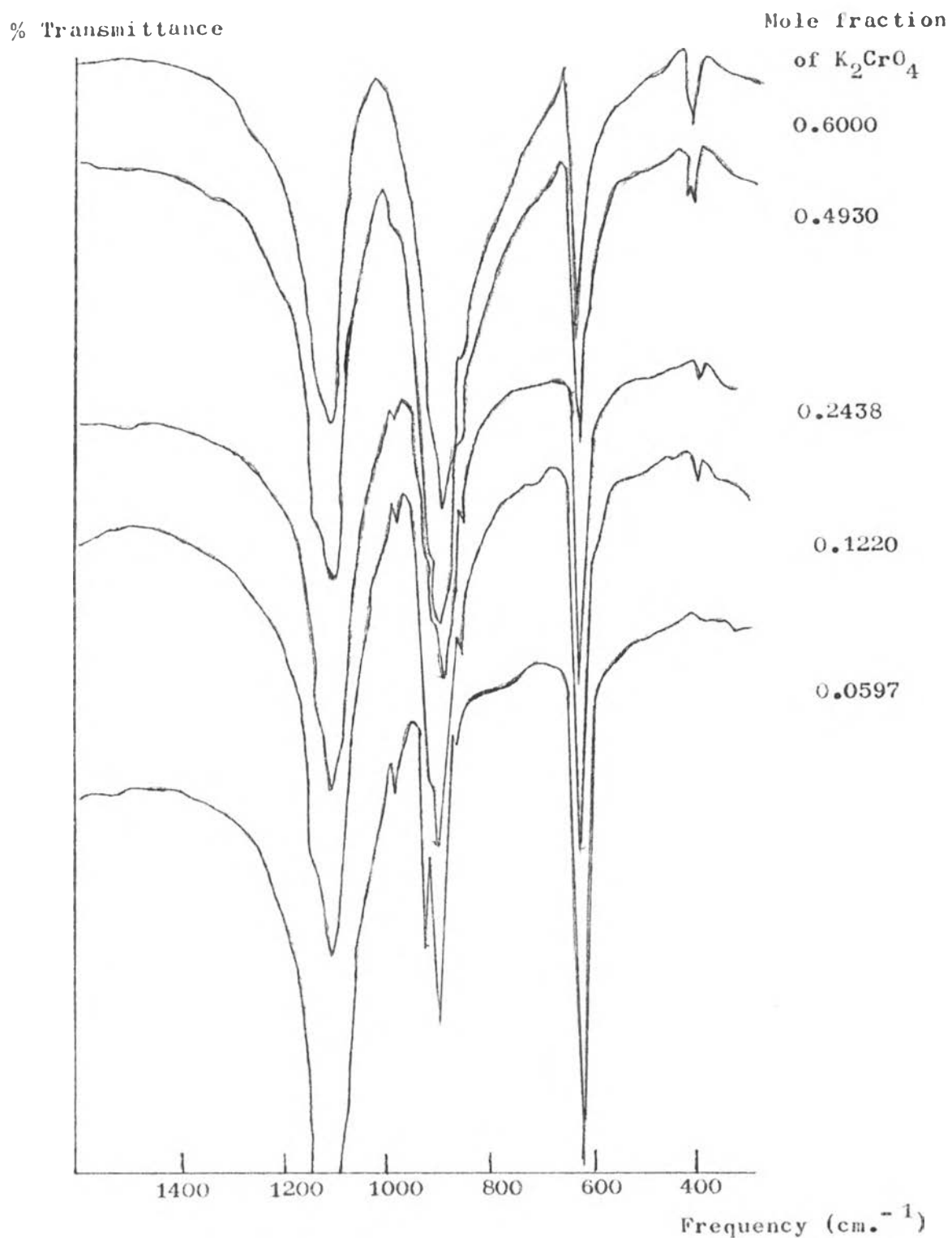


Figure 26 b The infrared spectra of  $K_2CrO_4/K_2SO_4$  mixed crystals.  
(cont.)

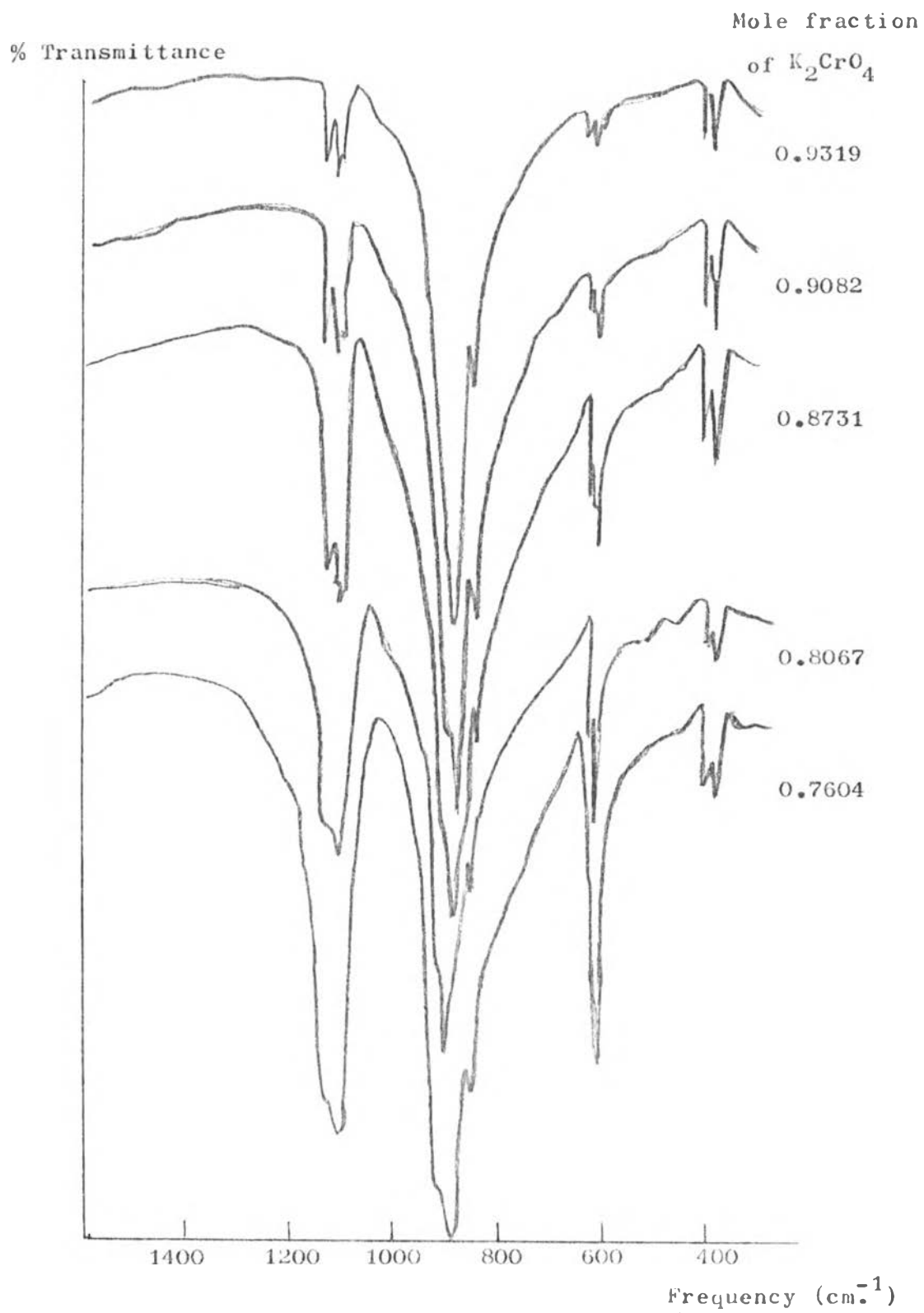


Figure 26c. The infrared spectra of  $K_2CrO_4/K_2SO_4$  mixed crystals.  
(cont.)

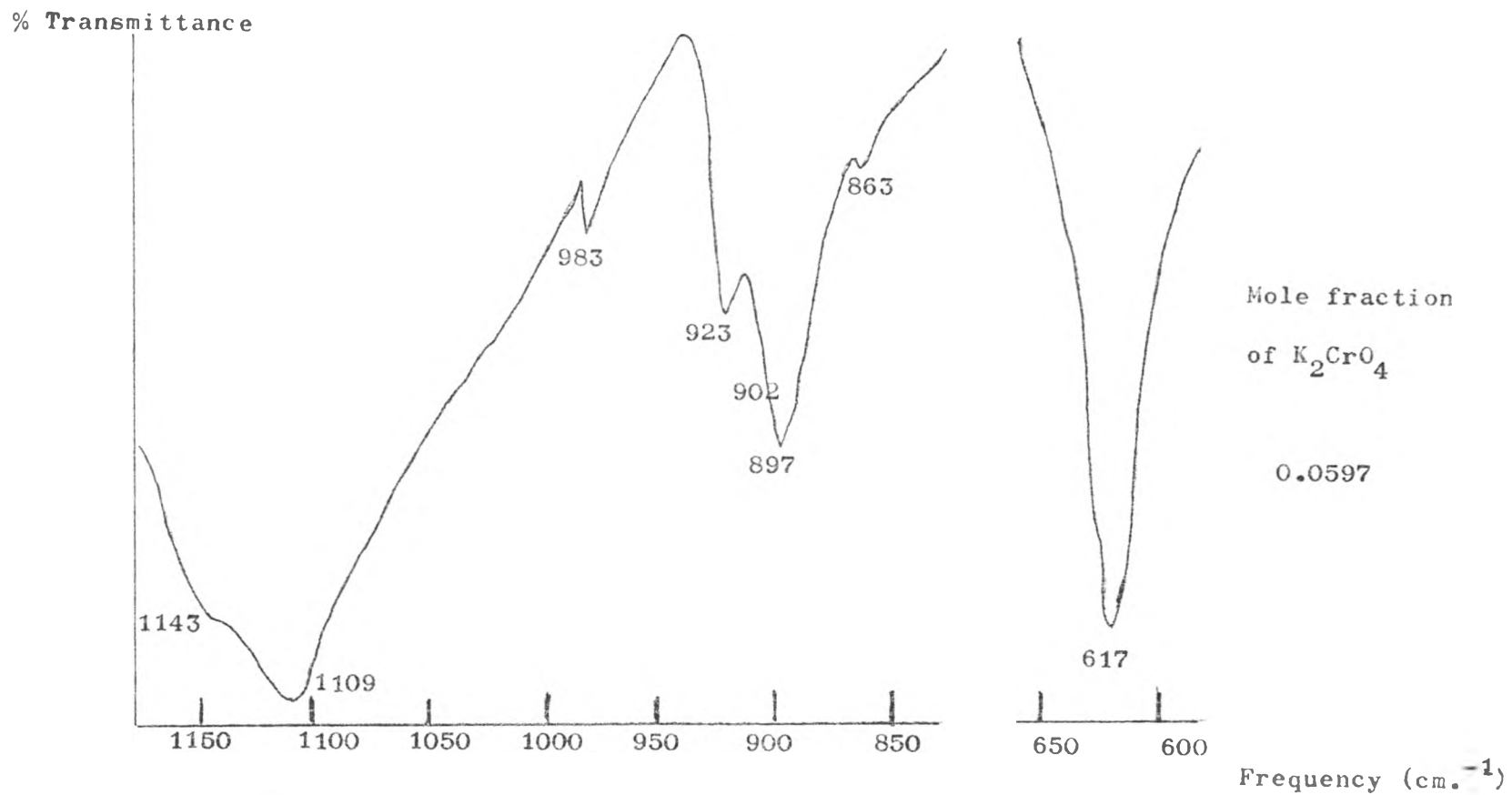


Figure 2d. The infrared spectra of the mixed crystal (expanded scale).

(cont.)

% Transmittance

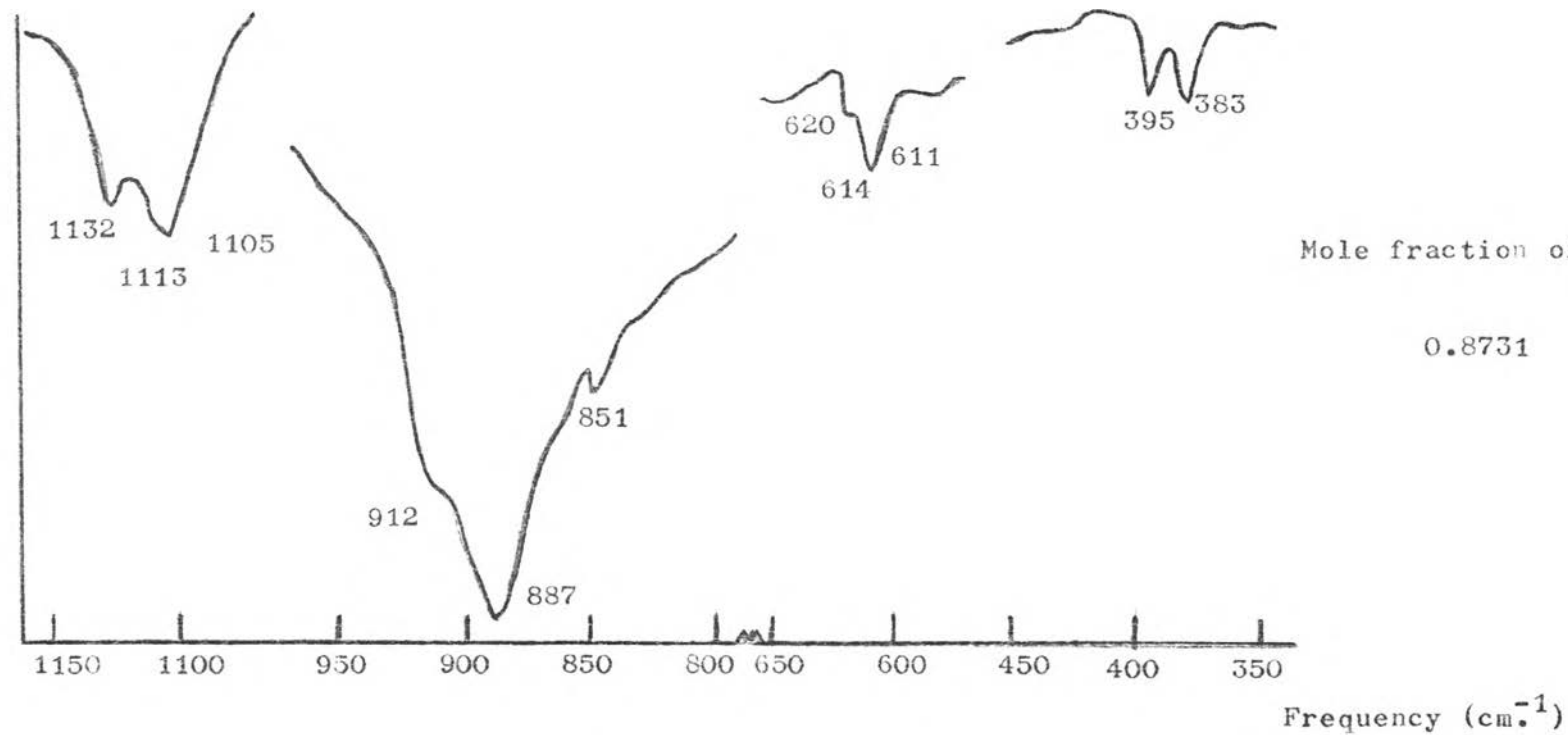


Figure 26e. The infrared spectra of the mixed crystals (expanded scale).

(cont.)

Table 36. Infrared frequencies ( $\text{cm}^{-1}$ ) of potassium chromate, potassium sulphate and mixed crystals

Mode	frequencies ( $\text{cm}^{-1}$ )									
	Pure $\text{K}_2\text{CrO}_4$	Pure $\text{K}_2\text{SO}_4$	$\text{K}_2\text{CrO}_4 / \text{K}_2\text{SO}_4$ mixed crystals							
			$x = 0.0115$ $y = 0.9885$	$0.0193$ $0.9807$	$0.0230$ $0.9770$	$0.0395$ $0.9605$	$0.0597$ $0.9403$	$0.1220$ $0.8780$	$0.2438$ $0.7562$	
$\nu_1$	851		-	863	865	863	863	863	859	859
		983	983	983	983	983	983	983	977	977
$\nu_2$	342		-	-	-	-	-	-	-	-
		-	-	-	-	-	-	-	-	-
$\nu_3$	887		897	897	897	897	897	897	887	887
	912		902	902	902	902	902	902	912	912
			923	923	923	923	923	923		
		1108	1108	1108	1108	1108	1108	1108	1108	1108
		1143	1143	1143	1143	1143	1143	1143	1143	1143
$\nu_4$	383		-	-	-	-	-	383	383	383
	395							395	395	395
		617	617	617	617	617	617	617	611	611
									620	620

Note x is mole fraction of  $\text{K}_2\text{CrO}_4$  in the mixed crystals  
y is mole fraction of  $\text{K}_2\text{SO}_4$  in the mixed crystals

Table 56. Infrared frequencies ( $\text{cm}^{-1}$ ) of potassium chromate, potassium sulphate and mixed crystals (cont.)

Mode	frequencies ( $\text{cm}^{-1}$ )								
	Pure $\text{K}_2\text{CrO}_4$	Pure $\text{K}_2\text{SO}_4$	$\text{K}_2\text{CrO}_4 / \text{K}_2\text{SO}_4$ mixed crystals.						
			x = 0.4930 y = 0.5070	0.6000	0.7604	0.8067	0.8731	0.9082	0.9319
$\nu_1$	851		859	851	851	851	851	851	851
		983	977	977	-	-	-	-	-
$\nu_2$	342		-	-	-	-	-	-	-
		-	-	-	-	-	-	-	-
$\nu_3$	887		887	887	887	887	887	887	887
	912		912	912	912	912	912	912	912
				1105	1105	1105	1105	1105	1105
		1108	1108	1113	1113	1113	1113	1113	1113
		1143	1143	1132	1132	1132	1132	1132	1132
$\nu_4$	383		385	383	383	383	383	383	383
	395		395	395	395	395	395	395	395
		617	611	611	611	611	611	611	611
			620	614	614	614	614	614	614
				620	620	620	620	620	620

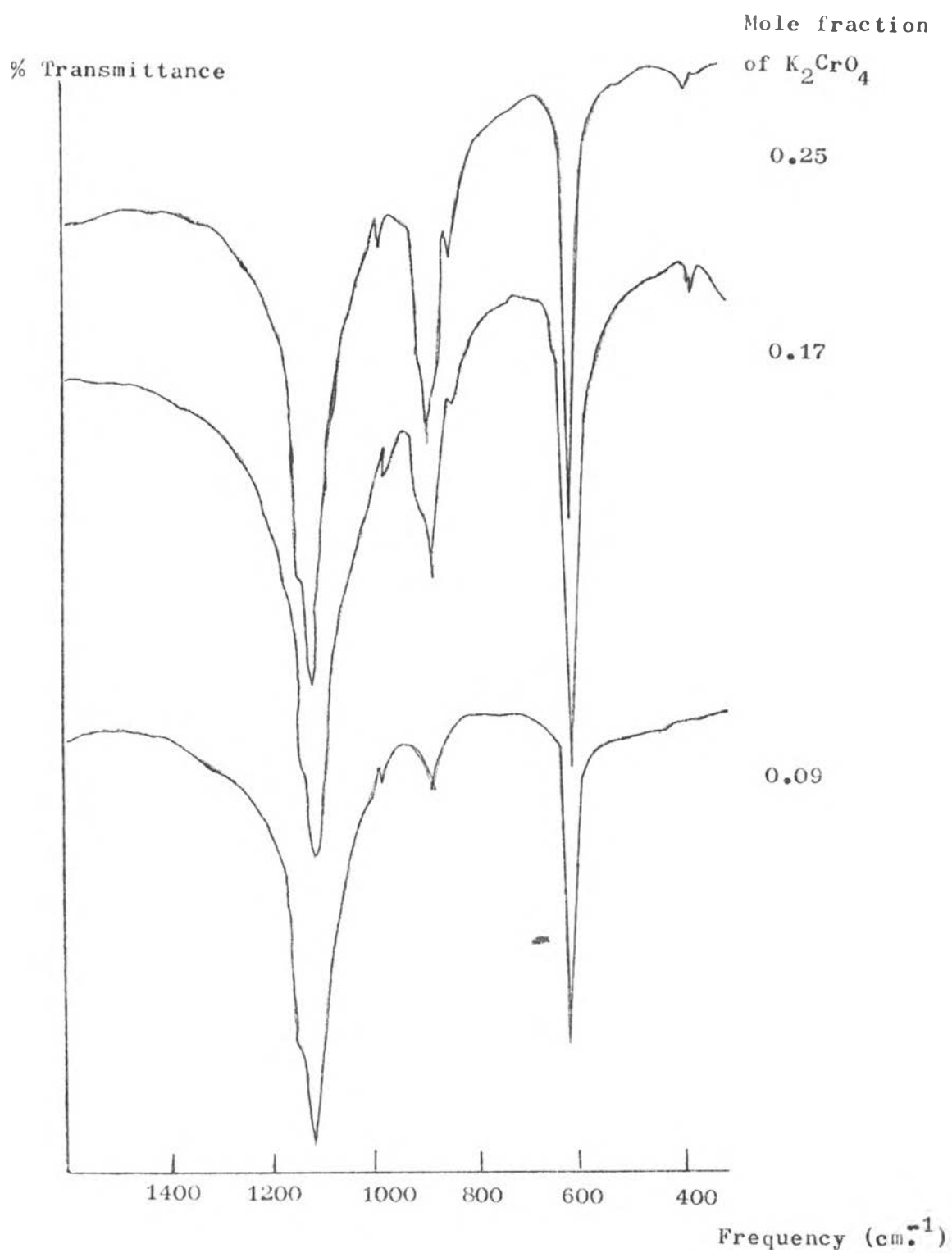


Figure 27a. The infrared spectra of the mixtures of potassium chromate and potassium sulphate

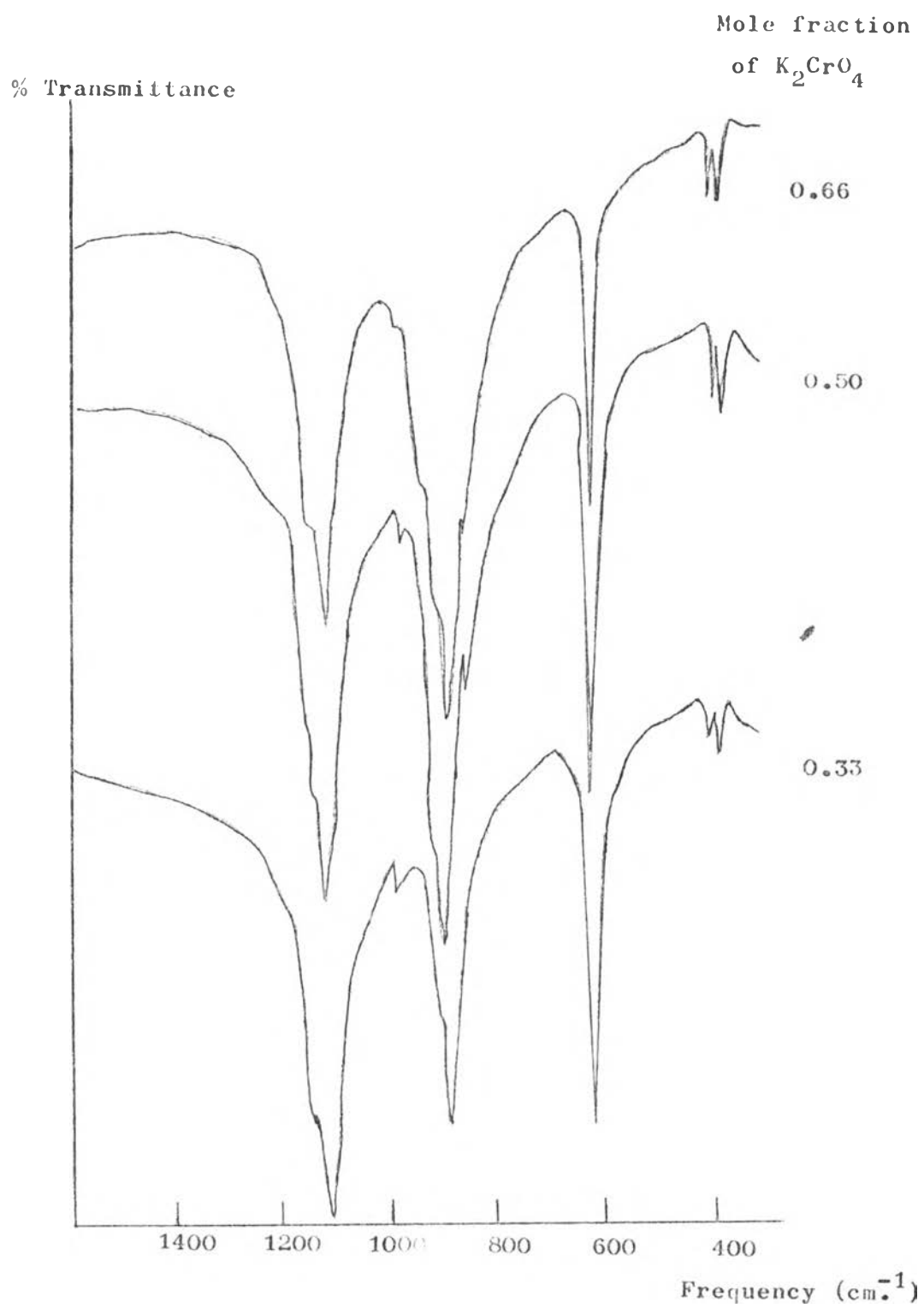


Figure 27b. The infrared spectra of the mixtures of  
(cont.) potassium chromate and potassium sulphate



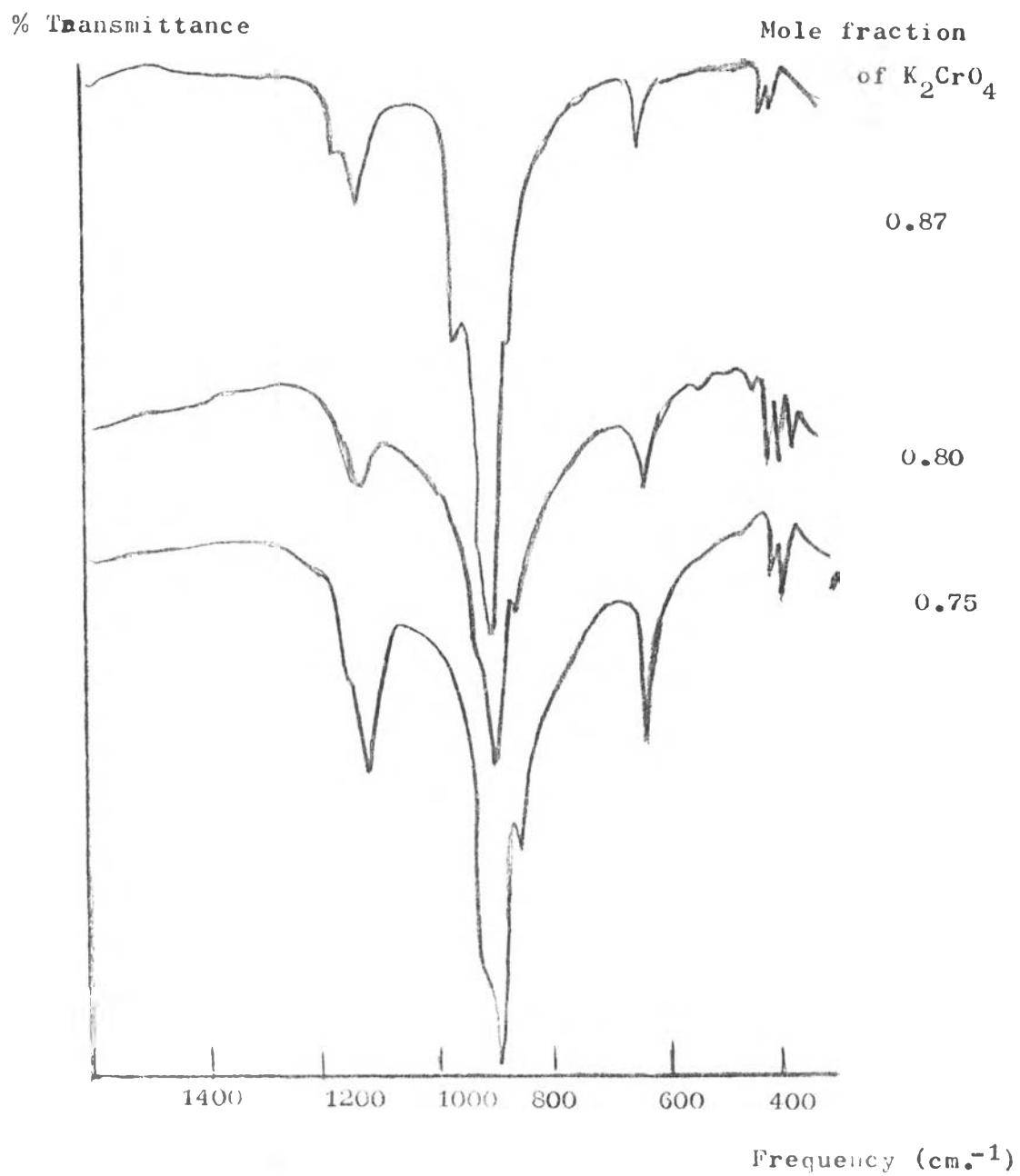


Figure 27c. The infrared spectra of the mixtures of  
(cont.) potassium chromate and potassium sulphate

### Infrared Spectra of Mixed Crystals.

The stretching mode  $\nu_1$ .

$\nu_1$  mode of potassium chromate at  $851 \text{ cm}^{-1}$  disappeared in the infrared spectra of mixed crystals at the low concentration about 0.01 mole fraction of potassium chromate. When the mole fraction of potassium chromate lay at 0.02-0.06, the frequency of this mode shifted to  $863 \text{ cm}^{-1}$ . The frequency was  $859 \text{ cm}^{-1}$  at the mole fraction 0.1-0.5 of potassium chromate, but changed to  $851 \text{ cm}^{-1}$  if the mole fraction was increased above 0.6.

$\nu_1$  mode of potassium sulphate at  $983 \text{ cm}^{-1}$  was present in the infrared spectra of mixed crystals in which the mole fraction of potassium chromate was about 0.01-0.06. At the mole fraction of potassium chromate around 0.1-0.6, the frequency shifted to  $977 \text{ cm}^{-1}$ . This mode disappeared when the mole fraction was above 0.7.

The doubly degenerate deformation mode  $\nu_2$ .

$\nu_2$  mode of potassium chromate disappeared in the infrared spectra of mixed crystals.

$\nu_2$  mode of potassium sulphate (not observed in this study but reported in reference 16) was also absent in the spectra of mixed crystals.

The triply degenerate stretching mode  $\nu_3$ .

$\nu_3$  mode of potassium chromate in the mixed crystals which the mole fraction of potassium chromate was 0.01-0.06 was splitted and shifted from  $887, 912, \text{cm}^{-1}$  to  $897, 902, 923 \text{ cm}^{-1}$ . But when the mole fraction of potassium chromate was above 0.1, the frequency was the same as of pure potassium chromate at  $887, 912 \text{ cm}^{-1}$ .

$\nu_3$  mode of potassium sulphate at 1108, 1143  $\text{cm}^{-1}$  was present in the spectra of mixed crystals in which the mole fraction of potassium chromate was 0.01-0.5. When the mole fraction of potassium chromate was above 0.6, the frequency was splitted and shifted to 1105, 1143, 1132  $\text{cm}^{-1}$ .

The triply degenerate deformation mode  $\nu_4$ .

$\nu_4$  mode of potassium chromate at 383, 395  $\text{cm}^{-1}$  disappeared in the spectra of mixed crystals in which the mole fraction of potassium chromate was 0.01-0.04. When the mole fraction of potassium chromate was above 0.06, this mode appeared at the same frequency as of pure potassium chromate.

$\nu_4$  mode of potassium sulphate at 617  $\text{cm}^{-1}$  was present in the spectra of mixed crystals in which the mole fraction of potassium chromate was 0.01-0.06. When the mole fraction of potassium chromate was 0.1-0.5, the frequency was splitted and shifted to 611, 620  $\text{cm}^{-1}$ . At the mole fraction above 0.6, the splitting was more pronounced at 611, 614, 620  $\text{cm}^{-1}$ .

## 2. Raman Spectra of Potassium Chromate/ Potassium Sulphate

### Mixed Crystals.

Raman spectra of the mixed crystals in various concentration compared with pure potassium chromate and pure potassium sulphate were shown in Figure 28. Their frequency data were reported in Table 37.

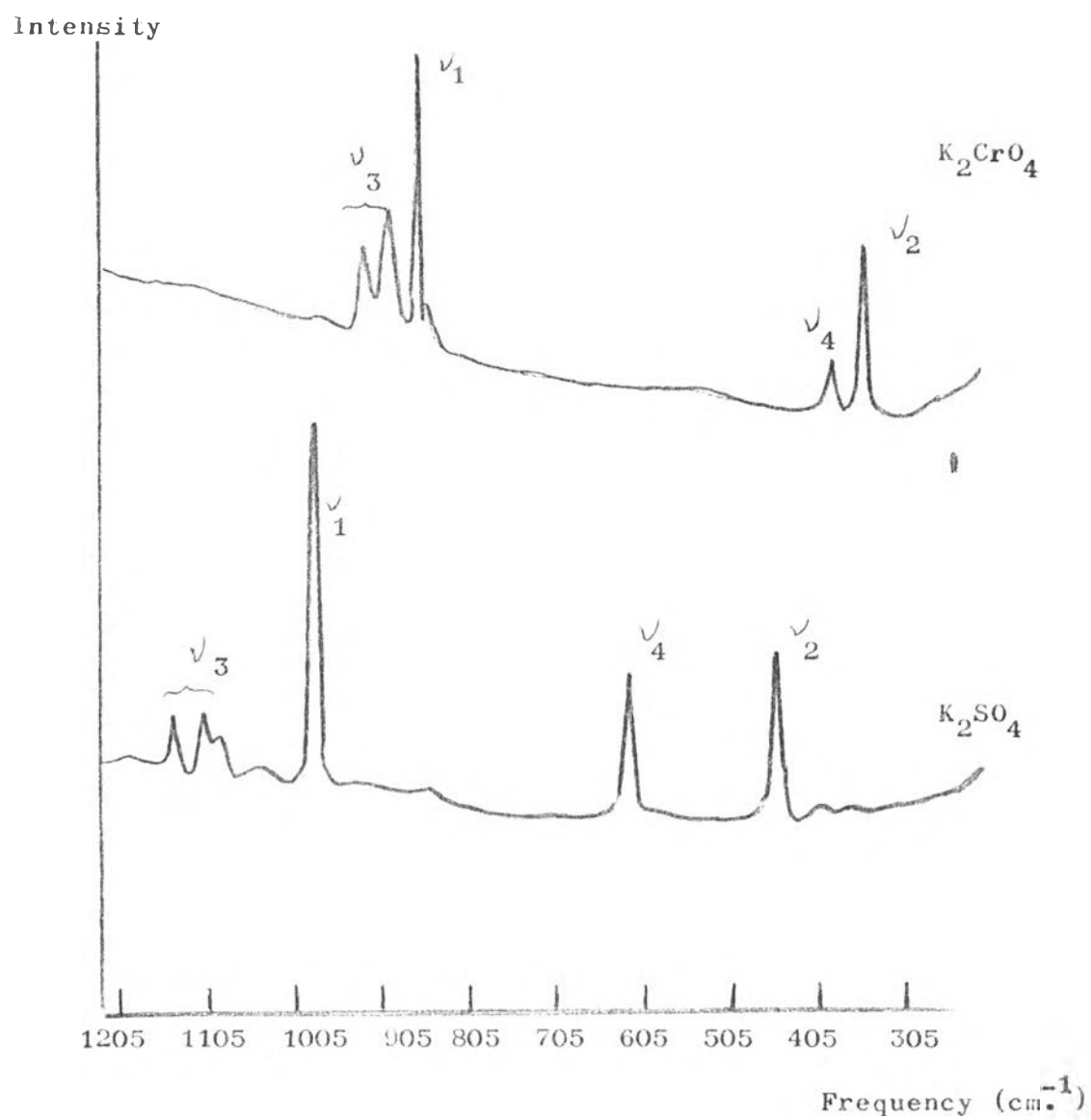


Figure 28. Raman spectra of potassium chromate, potassium sulphate (compared with the mixed crystals from the Figure 28 a, b, c)

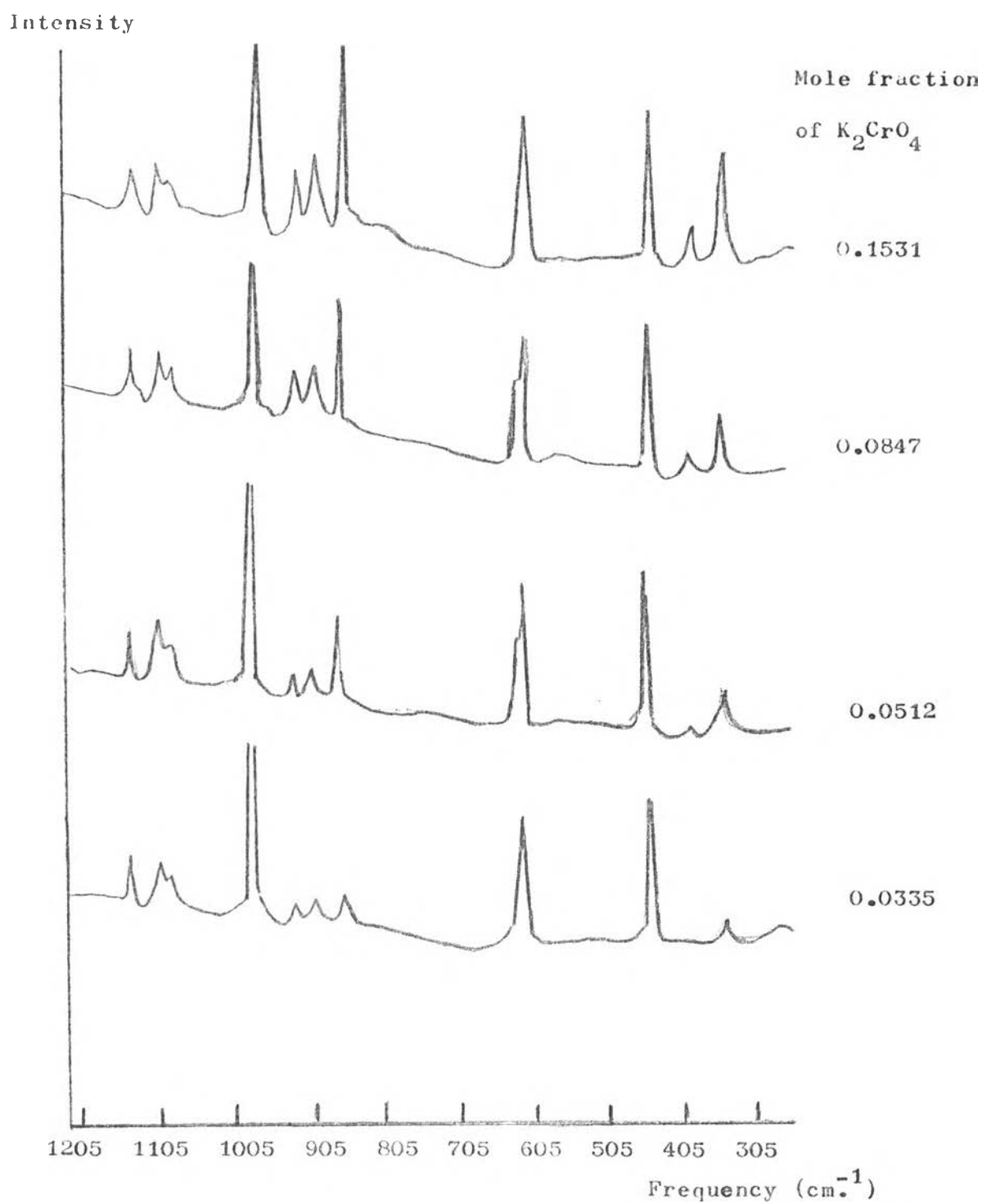


Figure 28a. Raman spectra of  $K_2CrO_4/K_2SO_4$  mixed crystals  
(cont.)

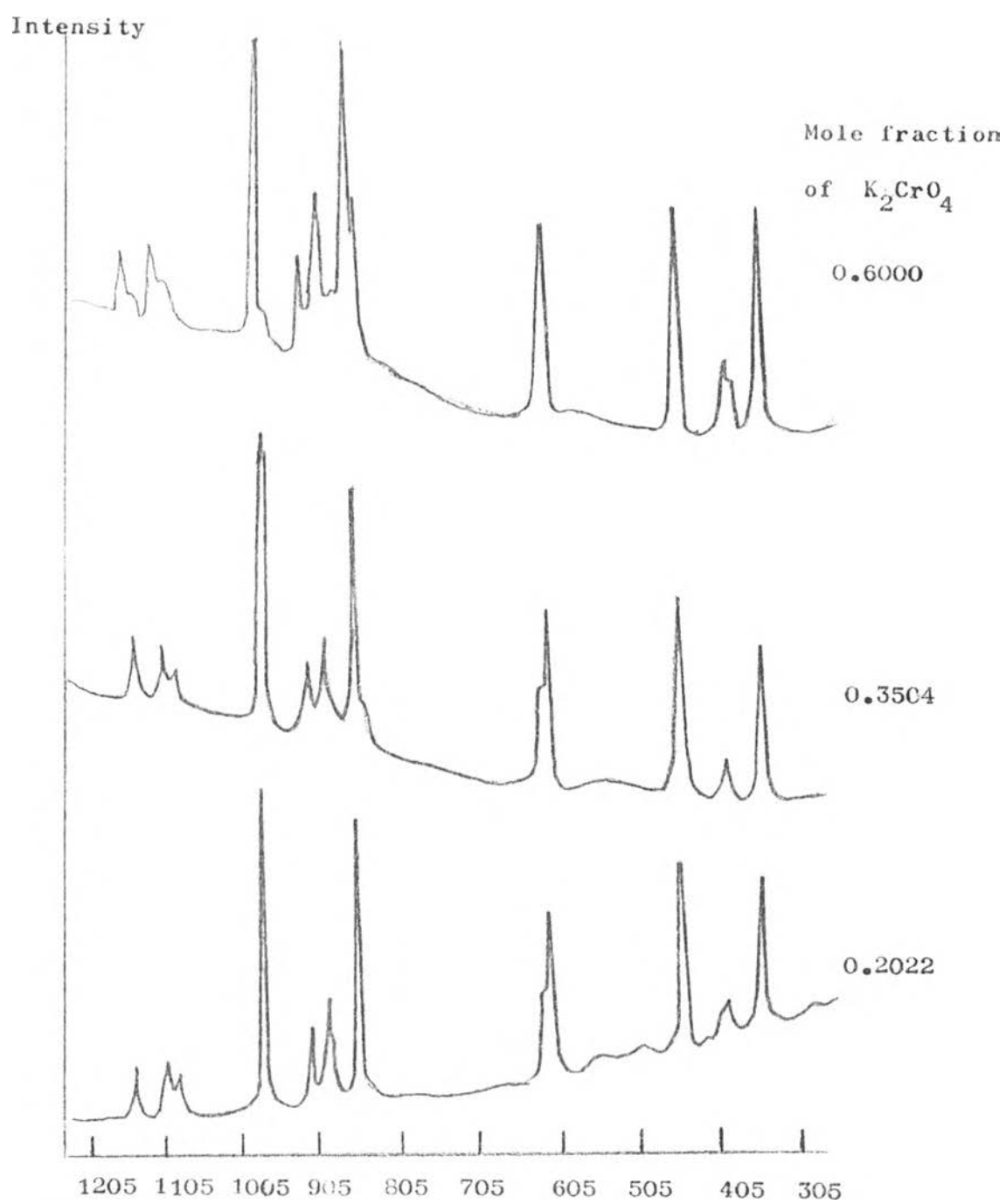


Figure 28 b. Raman spectra of  $K_2CrO_4/K_2SO_4$  mixed crystals.

(cont.)

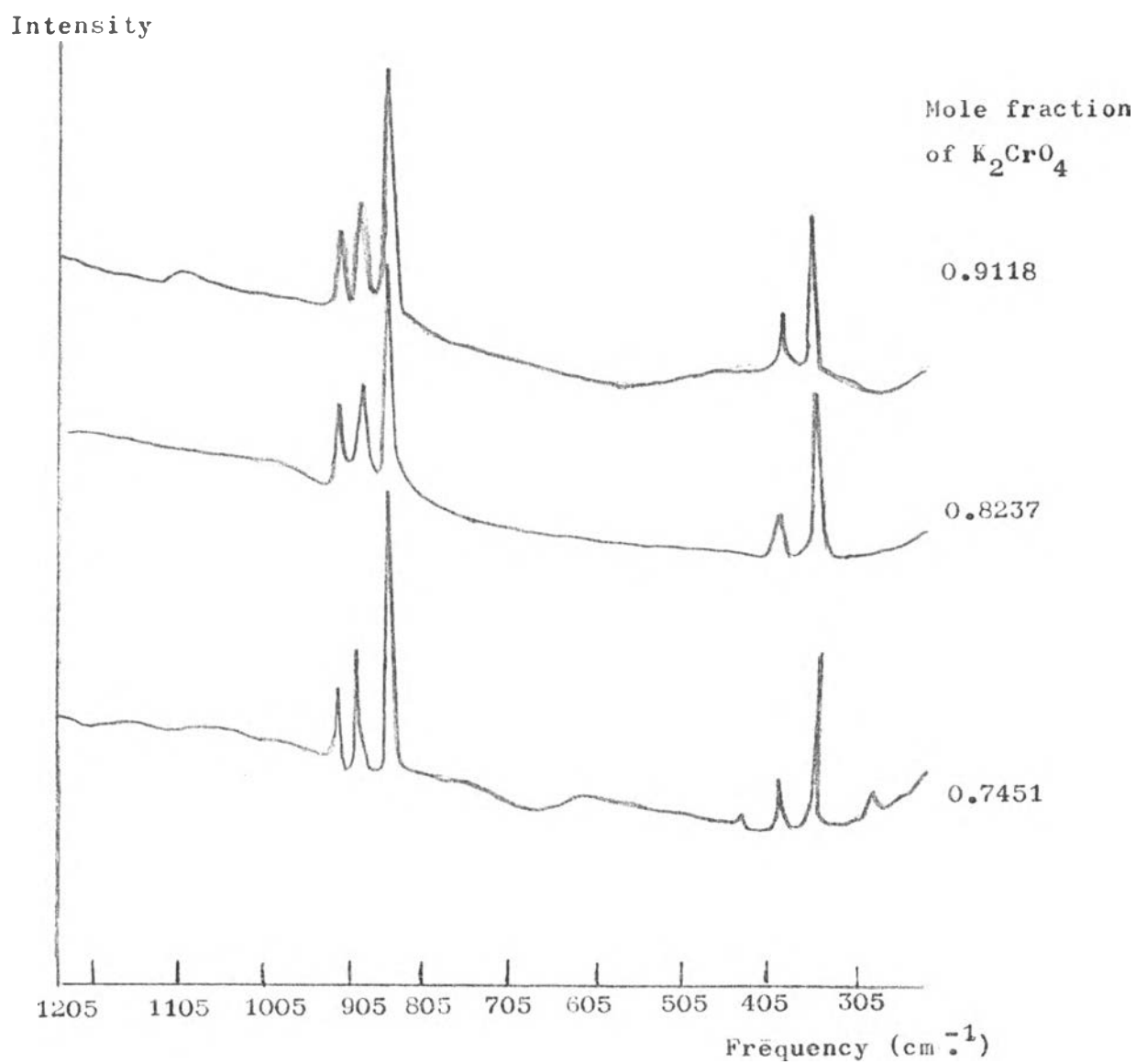


Figure 28c. Raman spectra of  $K_2CrO_4/K_2SO_4$  mixed crystals.

(cont.)

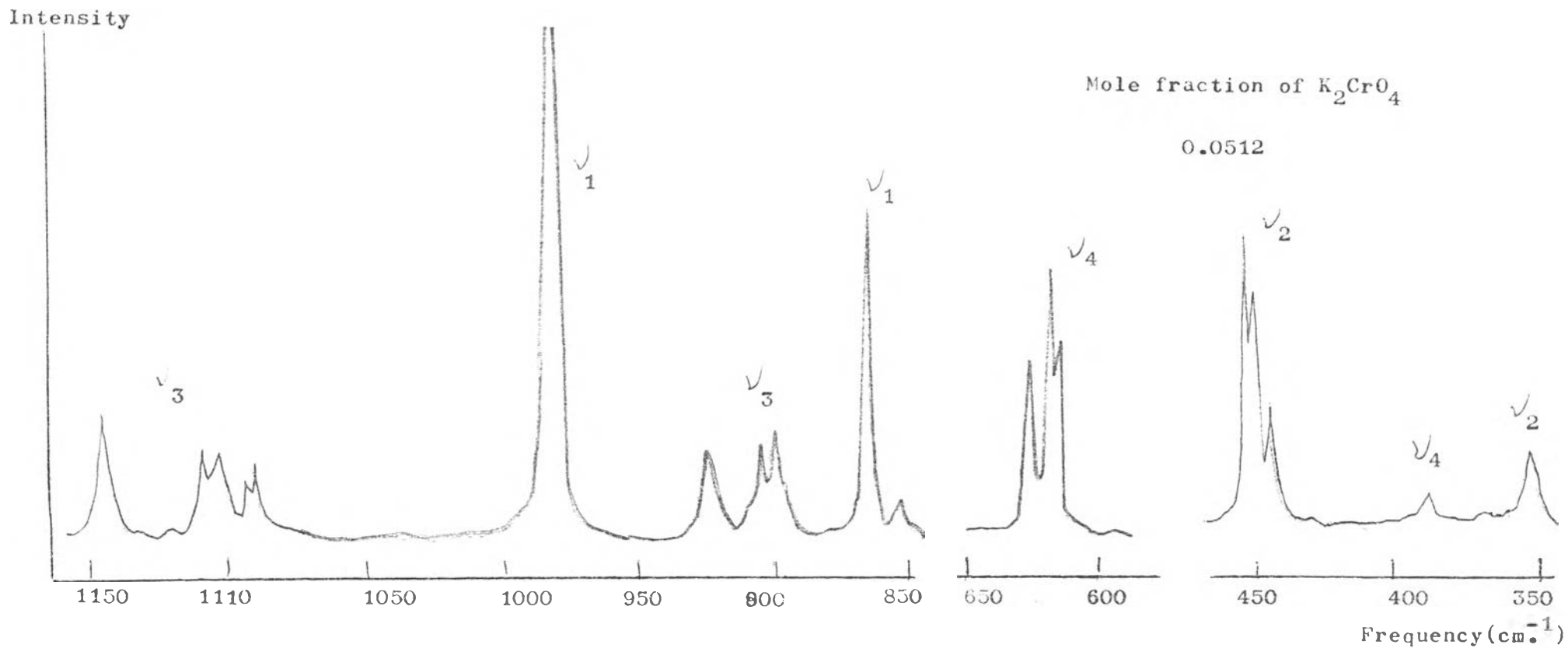


Figure 28 d. Raman spectrum of  $K_2CrO_4/K_2SO_4$  mixed crystals (expanded scale)  
(cont.)



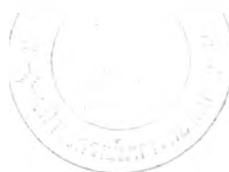
Table 37 - Raman frequencies ( $\text{cm}^{-1}$ ) of potassium chromate, potassium sulphate and mixed crystals

Mode	frequencies ( $\text{cm}^{-1}$ )								
	Pure $\text{K}_2\text{CrO}_4$	Pure $\text{K}_2\text{SO}_4$	$\text{K}_2\text{CrO}_4 / \text{K}_2\text{SO}_4$ mixed crystals.						
			x = 0.0355 y = 0.9665	0.0512 0.9488	0.0847 0.9153	0.1531 0.8469	0.2022 0.7978	0.3504 0.6496	0.6000 0.4000
$\nu_1$	847		867.5	867.5	867.5	867.5	867.5	867.5	867.5
		983	983	983	983	983	983	983	983
$\nu_2$	344		344	344	344	344	344	344	344
		447	447	447	447	447	447	447	447
		453	453	453	453	453	453	453	453
		457	457	457	457	457	457	457	457
$\nu_3$	862		902	902	902	902	902	902	902
	872		906	906	906	906	906	906	906
	898		926	926	926	926	926	926	926
		1093	1093	1093	1093	1093	1093	1093	1093
		1105	1105	1105	1105	1105	1105	1105	1105
		1110	1110	1110	1110	1110	1110	1110	1110
		1145	1145	1145	1145	1145	1145	1145	1145
$\nu_4$	382		382	382	382	382	382	382	382
	389		389	389	389	389	389	389	389
	392		392	392	392	392	392	392	392
		616	616	616	616	616	616	616	616
		620	620	620	620	620	620	620	620
		628.5	628.5	628.5	628.5	628.5	628.5	628.5	628.5

Table 37. Raman frequencies ( $\text{cm}^{-1}$ ) of potassium chromate, potassium sulphate and mixed crystals. (cont.)

Mode	frequencies ( $\text{cm}^{-1}$ )				
	Pure $\text{K}_2\text{CrO}_4$	Pure $\text{K}_2\text{SO}_4$	$\text{K}_2\text{CrO}_4 / \text{K}_2\text{SO}_4$ mixed crystals.		
			$x = 0.7451$ $y = 0.2549$	0.8237 0.1763	0.9118 0.0882
$\nu_1$	847		847	847	847
		983	-	-	-
$\nu_2$	344		344	344	344
		447	-	-	-
		453	-	-	-
		457	-	-	-
$\nu_3$	862		862	862	862
	872		872	872	872
	898		898	898	898
		1093	-	-	-
		1105	-	-	-
		1110	-	-	-
		1145	-	-	-
$\nu_4$	382		382	382	382
	389		389	389	389
	392		392	392	392
		616	-	-	-
		620	-	-	-
		628.5	-	-	-

Raman Spectra of Mixed Crystals



The stretching mode  $\nu_1$ .

$\nu_1$  mode of potassium chromate in the mixed crystals which was studied from the dilution limit to 0.6 mole fraction of potassium chromate, shifted from  $847 \text{ cm}^{-1}$  to  $867.5 \text{ cm}^{-1}$ . When the mole fraction of potassium chromate was increased, the frequency of this mode was  $847 \text{ cm}^{-1}$ .

$\nu_1$  mode of potassium sulphate at  $983 \text{ cm}^{-1}$  was present in Raman spectra of mixed crystals. When the mole fraction of potassium chromate was above 0.7, it disappeared.

The doubly degenerate deformation mode  $\nu_2$ .

$\nu_2$  mode of potassium chromate at  $344 \text{ cm}^{-1}$  was present in Raman spectra of mixed crystals in every concentration.

$\nu_2$  mode of potassium sulphate at  $447, 453, 457 \text{ cm}^{-1}$  was present in Raman spectra of mixed crystals, studied from the dilution limit to 0.6 mole fraction of potassium chromate. The frequency disappeared when the mole fraction of potassium chromate was increased above 0.7 .

The triply degenerate stretching mode  $\nu_3$ .

$\nu_3$  mode of potassium chromate in the mixed crystals which was studied from the dilution limit to 0.6 mole fraction of potassium chromate shifted from  $862, 872, 898 \text{ cm}^{-1}$  to  $902, 906, 926 \text{ cm}^{-1}$ . When the mole fraction was increased, this mode was at the same frequency as of pure potassium chromate ( $862, 872, 898 \text{ cm}^{-1}$ )

$\nu_3$  mode of potassium sulphate at  $1093, 1105, 1110 \text{ cm}^{-1}$  was present in the spectra of mixed crystals. It disappeared when the mole fraction of potassium chromate was above 0.7 .

The triply degenerate deformation mode  $\nu_4$ .

$\nu_4$  mode of potassium chromate at 382, 389, 392  $\text{cm}^{-1}$  was present in the spectra of mixed crystals in every concentration.

$\nu_4$  mode of potassium sulphate at 616, 620, 628.5  $\text{cm}^{-1}$  was present in the spectra of mixed crystals but disappeared when the mole fraction of potassium chromate was above 0.7 .

If the major interaction between anions was assumed to be due to long range dipolar coupling and the dipolar coupling between like anions was much greater than between unlike anions, then the addition of impurities would decrease the dipolar coupling between host ions, and a frequency shift should result. Modes of different symmetry should have different frequency shift as the nature of the dipolar coupling was different in modes of different symmetry.

As in Table 37 indicated, Raman frequency of  $\nu_1$  mode of potassium chromate shifted from 847  $\text{cm}^{-1}$  to 867.5  $\text{cm}^{-1}$  in the mixed crystals. The frequency shift was 20  $\text{cm}^{-1}$ .

Raman frequency of  $\nu_3$  mode of potassium chromate in the mixed crystals in dilution limit shifted from 862, 872, 898  $\text{cm}^{-1}$  to 902, 906, 926  $\text{cm}^{-1}$ . The separation of frequencies ( between 862 and 898  $\text{cm}^{-1}$ ) of pure potassium chromate was 36  $\text{cm}^{-1}$ , but the separation of frequencies ( between 902 and 926  $\text{cm}^{-1}$ ) of mixed crystals was 24  $\text{cm}^{-1}$  as shown in Table 38 . The decrease in separation from pure potassium chromate to the dilution limit ( 36-24 = 12  $\text{cm}^{-1}$ ) was the magnitude of the factor group effects.

Table 53. Raman frequencies ( $\text{cm}^{-1}$ ) in the  $\nu_3$  mode of potassium chromate and of mixed crystals.

Mode	Frequencies ( $\text{cm}^{-1}$ )		
	Pure $\text{K}_2\text{CrO}_4$	$\text{K}_2\text{CrO}_4/\text{K}_2\text{SO}_4$ Mixed crystals	Factor group splitting, $\Delta\nu_f$
$\nu_3$	862 872 898 } $\Delta\nu_f = 36$	902 906 926 } $\Delta\nu_f = 24$	12

### X-ray Powder Diffraction Data

The X-ray powder diffraction were recorded as both photographs in film method and diffractograms in diffractometer method.

In film method, it was difficult to read precisely the positions of the  $2\theta$  angle and the relative intensity of diffracted beams. So the X-ray powder diffraction data reported in this study were taken from diffractograms in diffractometer method only.

The positions of the  $2\theta$  angle were corrected by comparing with the peaks of silicon which acted as internal standard.

#### 1. The X-ray Powder Diffraction Data of Potassium Chromate.

The X-ray powder diffraction data of potassium chromate were reported in Table 39. The diffractogram of potassium chromate was shown in Figure 29.

Table 39. The observed  $2\theta$  of potassium chromate.

line	hkl	observed		reference (35)	
		$2\theta$ ( $^{\circ}$ )	d ( $\text{\AA}$ )	$2\theta$ ( $^{\circ}$ )	d ( $\text{\AA}$ )
1	020	17.10	5.180	17.23	5.200
2	120	20.85	4.257	20.99	4.299
3	200	23.30	3.814	23.69	3.834
4	210	25.70	3.536	25.39	3.593
5	201	28.60	3.119	28.62	3.216
6	220	29.10	3.066	30.03	3.078
7	031	29.92	2.984	31.04	2.988
8	002	30.25	2.952	31.36	2.960
9	221	34.55	2.594	34.31	2.733
10	112	35.00	2.562	35.29	2.667
11	040	36.25	2.476	36.35	2.599
12	230	36.90	2.434	36.83	2.570
13	122	39.45	2.282	39.19	2.438

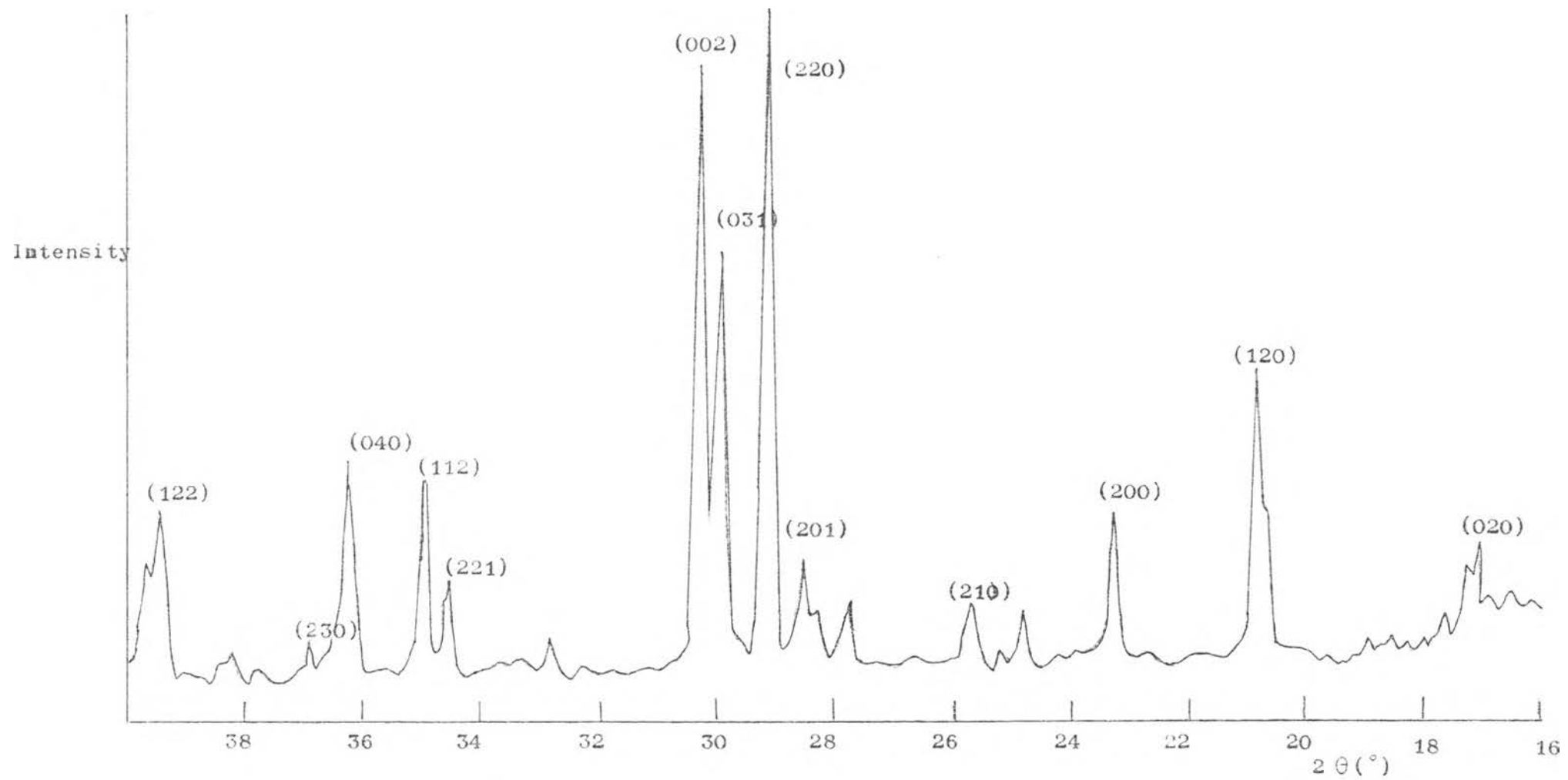


Figure 29. The diffractogram of potassium chromate

### 1.1 The Determination of Unit Cell Parameters by Least Square Method.

In orthorhombic system, the interplanar spacing  $d_{hkl}$ , the Bragg angle  $\theta$  are related with the plane indices (hkl) and the lattice constants (a,b,c) as in the following :

$$\left(\frac{1}{2d}\right)^2 = \left(\frac{\sin \theta}{\lambda}\right)^2 = A h^2 + B k^2 + C l^2$$

where

$$\begin{aligned} A &= \frac{1}{4 a^2} \\ B &= \frac{1}{4 b^2} \\ C &= \frac{1}{4 c^2} \end{aligned}$$

It was shown in Appendix B. that A, B and C can be found from three equations :

$$\begin{aligned} A [P U - Q V] + C [T U - V W] &= Y U - Z V \\ A [Q X - U W] + B [U X - R W] &= Z X - S W \\ B [V U - R P] + C [T U - X P] &= Y U - S P \end{aligned}$$

$$\begin{aligned} \text{where} \quad \sum h^2 &= P \\ \sum h^4 &= Q \\ \sum k^2 &= V \\ \sum k^4 &= R \\ \sum l^2 &= T \\ \sum (h^2 k^2) &= U \\ \sum (h^2 l^2) &= W \\ \sum (k^2 l^2) &= X \\ \sum \left(\frac{\sin \theta}{\lambda}\right)^2 &= Y \\ \sum \left(\frac{\sin \theta \cdot h}{\lambda}\right)^2 &= Z \\ \sum \left(\frac{\sin \theta \cdot k}{\lambda}\right)^2 &= S \end{aligned}$$



Table 40. The various terms in the determination of unit cell parameters of potassium chromate.

hkl	$\left(\frac{\sin \theta}{\lambda}\right)^2$	$\left(\frac{\sin \theta h}{\lambda}\right)^2$	$\left(\frac{\sin \theta k}{\lambda}\right)^2$	$h^2$	$h^4$	$k^2$	$k^4$	$l^2$	$h^2 k^2$	$h^2 l^2$	$k^2 l^2$
020	0.0093	0	0.0372	0	0	4	16	0	0	0	0
120	0.0138	0.0138	0.0552	1	1	4	16	0	4	0	0
200	0.0172	0.0688	0	4	16	0	0	0	0	0	0
210	0.0208	0.0832	0.0208	4	16	1	1	0	4	0	0
201	0.0257	0.1028	0	4	16	0	0	1	0	4	0
220	0.0266	0.1064	0.1064	4	16	4	16	0	16	0	0
031	0.0281	0	0.2529	0	0	9	81	1	0	0	9
002	0.0287	0	0	0	0	0	0	4	0	0	0
221	0.0372	0.1488	0.1488	4	16	4	16	1	16	4	4
112	0.0381	0.0381	0.0381	1	1	1	1	4	1	4	4
040	0.0403	0	0.6528	0	0	16	256	0	0	0	0
230	0.0422	0.1688	0.3798	4	16	9	81	0	36	0	0
122	0.0480	0.0480	0.1920	1	1	4	16	4	4	4	16
$\Sigma =$	0.3765	0.7787	1.8840	27	99	56	500	15	81	16	33
	Y	Z	S	P	Q	V	R	T	U	W	X

Note:  $\lambda = 1.5405 \text{ \AA}$

Using three equations described above , the results were :

$$\begin{aligned}
 A &= 4.581 \times 10^{-3} \\
 \therefore a &= 7.387 \text{ \AA} \\
 B &= 2.529 \times 10^{-3} \\
 \therefore b &= 9.942 \text{ \AA} \\
 C &= 7.100 \times 10^{-3} \\
 \therefore c &= 5.934 \text{ \AA}
 \end{aligned}$$

Table 41. The unit cell parameters of potassium chromate by least square method.

Unit cell parameters	observed (\AA)	reference(35) (\AA)
a	7.387	7.663
b	9.942	10.391
c	5.934	5.919

### 1.2 The Determination of Unit Cell Parameters by Unique Value Method.

The unit cell parameters a, b, c were determined from only three lines having indices 200, 020 and 002 .

$$\left( \frac{\sin \theta}{\lambda} \right)_{hkl}^2 = A h^2 + B k^2 + C l^2$$

$$A = \left( \frac{\sin \theta}{2 \lambda} \right)_{200}^2$$

$$B = \left( \frac{\sin \theta}{2 \lambda} \right)_{020}^2$$

$$C = \left( \frac{\sin \theta}{2 \lambda} \right)_{002}^2$$

Table 42. The unit cell parameters of potassium chromate by the unique value method.

Unit cell parameters	Observed (Å)	Reference (Å) (35)
a	7.628	7.663
b	10.363	10.391
c	5.903	5.919

The unit cell parameters of potassium chromate determined by two methods: the least square method and the unique value method: were compared with the reference 35 in Table 43. It was seen that the results taken from the unique value method were closer to the reference than from the least square method.

Table 43. The unit cell parameters of potassium chromate from two methods.

Unit cell parameters	Observed (Å)		Reference (35) (Å)
	Method		
	Least square	Unique value	
a	7.387	7.628	7.663
b	9.942	10.363	10.391
c	5.934	5.903	5.919

## 2. The X-ray Powder Diffraction Data of Potassium Sulphate.

The X-ray powder diffraction data of potassium sulphate were reported in Table 44. The diffractogram of potassium sulphate was shown in Figure 30 .

Table 44. The observed  $2\theta$  of potassium sulphate.

line	hkl	observed		reference (36)	
		$2\theta$ ( $^{\circ}$ )	d (Å)	$2\theta$ ( $^{\circ}$ )	d (Å)
1	020	17.60	5.035	17.84	5.030
2	120	21.30	4.168	21.65	4.176
3	200	23.80	3.735	24.30	3.743
4	210	26.30	3.386	26.05	3.508
5	201	29.20	3.056	29.38	3.140
6	220	29.80	2.996	30.89	3.001
7	031	30.80	2.901	32.05	2.903
8	002	31.00	2.882	32.26	2.886
9	221	35.60	2.520	35.32	2.665
10	112	36.00	2.493	36.30	2.602
11	040	37.80	2.378	37.72	2.518
12	230	38.00	2.366	38.06	2.499
13	122	40.40	2.231	40.46	2.374

The procedure in determining the unit cell parameters of potassium sulphate was the same as of potassium chromate. The results were summarized in Table 45 .

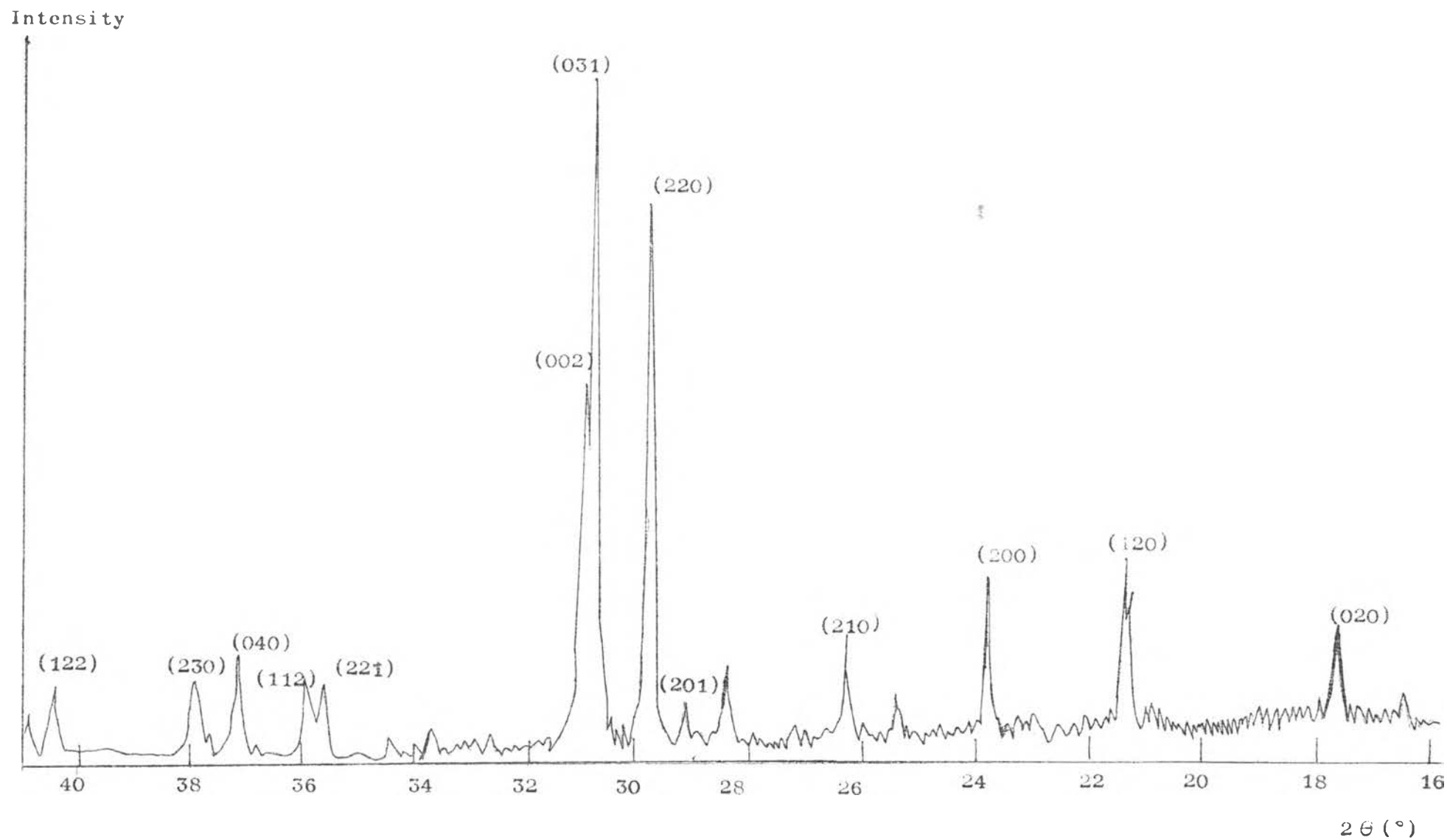


Figure 30. The diffractogram of potassium sulphate.

Table 45 The unit cell parameters of potassium sulphate from two methods.

Unit cell parameters	Observed ( Å )		Reference (36)
	Method		
	Least square	Unique value	( Å )
a	7.220	7.483	7.468
b	9.551	10.072	10.070
c	5.810	5.772	5.764

It was seen that the results taken from the unique value method were closer to the reference than the least square method.

In the least square method, the positions of 13 peaks were refined to give the best values of the unit cell parameters a, b and c. From Table 39,44 it was seen that the positions of peaks in high-angle regions deviated from those in reference 35,36. The deviation in this study was supported by the data (diffractogram) of potassium sulphate obtained by the same instrument in reference 37. Therefore, the unit cell parameters obtained from the least square method were markedly different from those of reference 35,36. The unique value method gave closer results to reference 35,36 though it was not a statistical method.

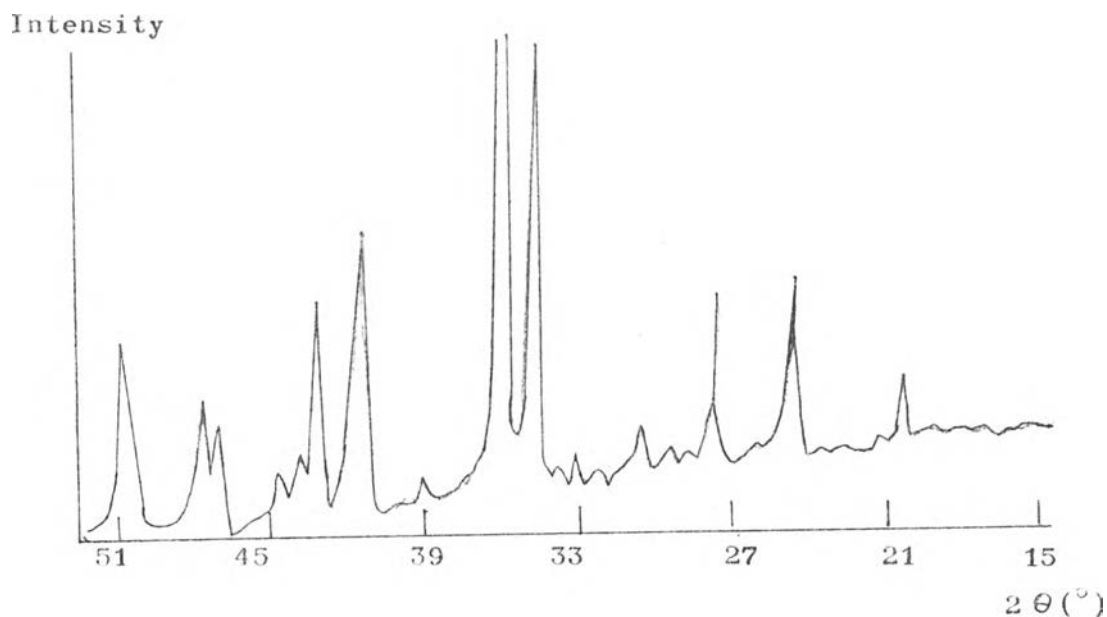


Figure 31. The diffractogram of potassium sulphate taken from reference 37.

### 3. The X-ray Powder Diffraction Data of Potassium Chromate/ Potassium Sulphate Mixed Crystals.

The X-ray powder diffraction data of the mixed crystals were reported in Table 46. The diffractogram of mixed crystals were shown in Figure 32.

The diffractograms of the mixed crystals were different from pure crystals. The mixed crystal gave a diffraction pattern which was intermediate, in respect of both the positions and the intensities of the peaks, between those of the pure crystals.

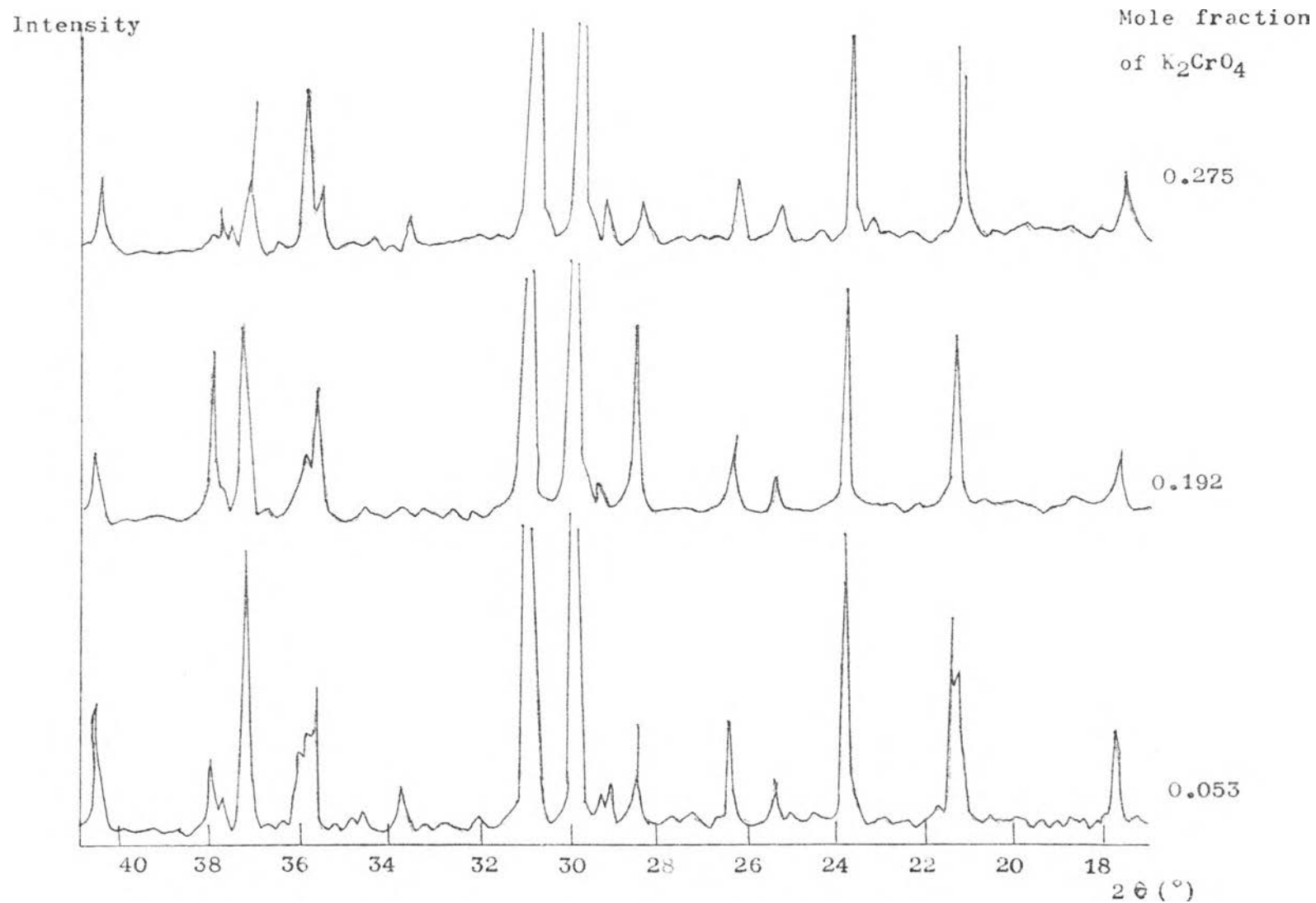


Figure 32a. The diffractograms of  $K_2CrO_4/K_2SO_4$  mixed crystals



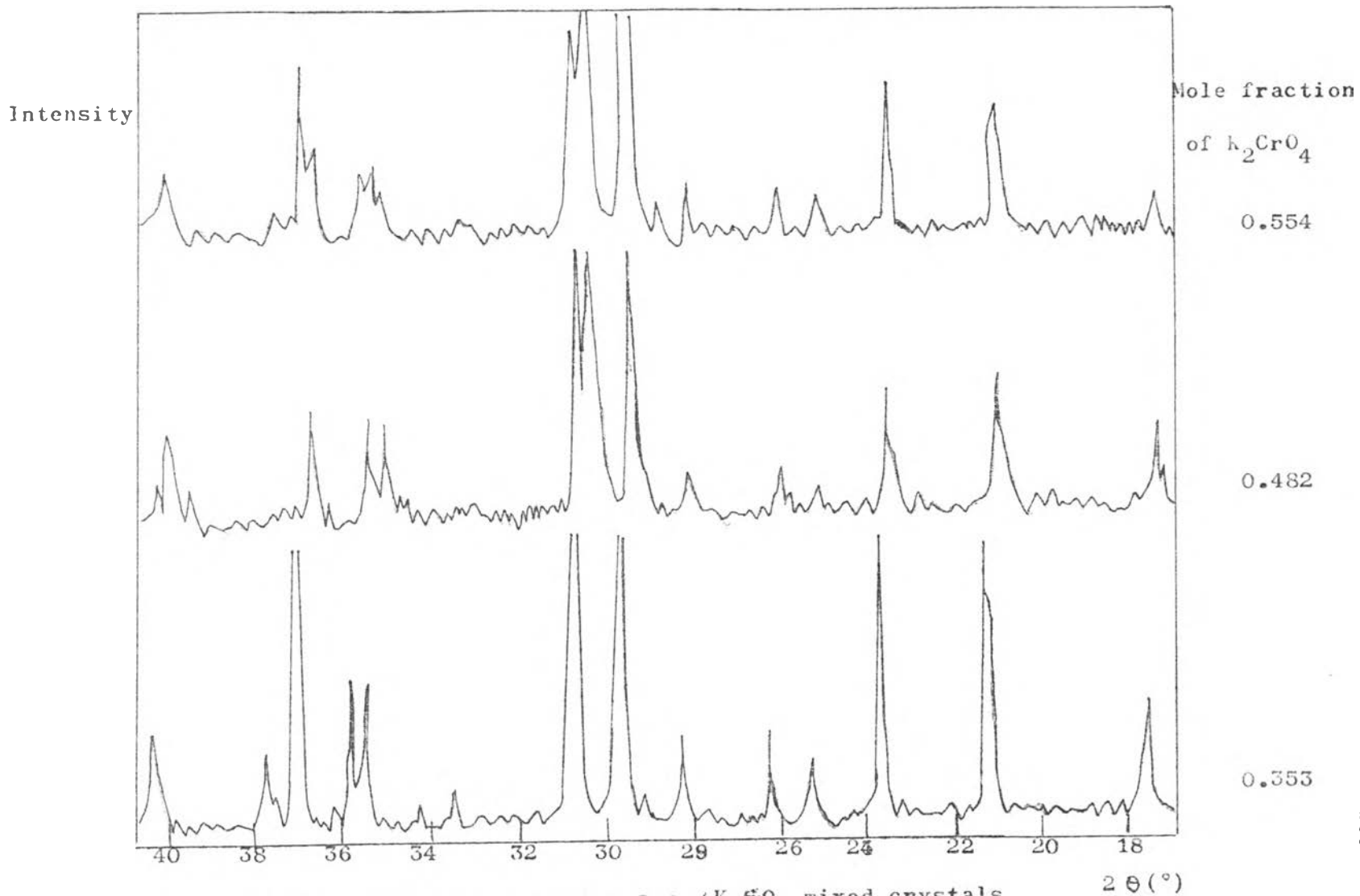


Figure 32b. The diffractograms of  $K_2CrO_4/K_2SO_4$  mixed crystals  
(cont.)

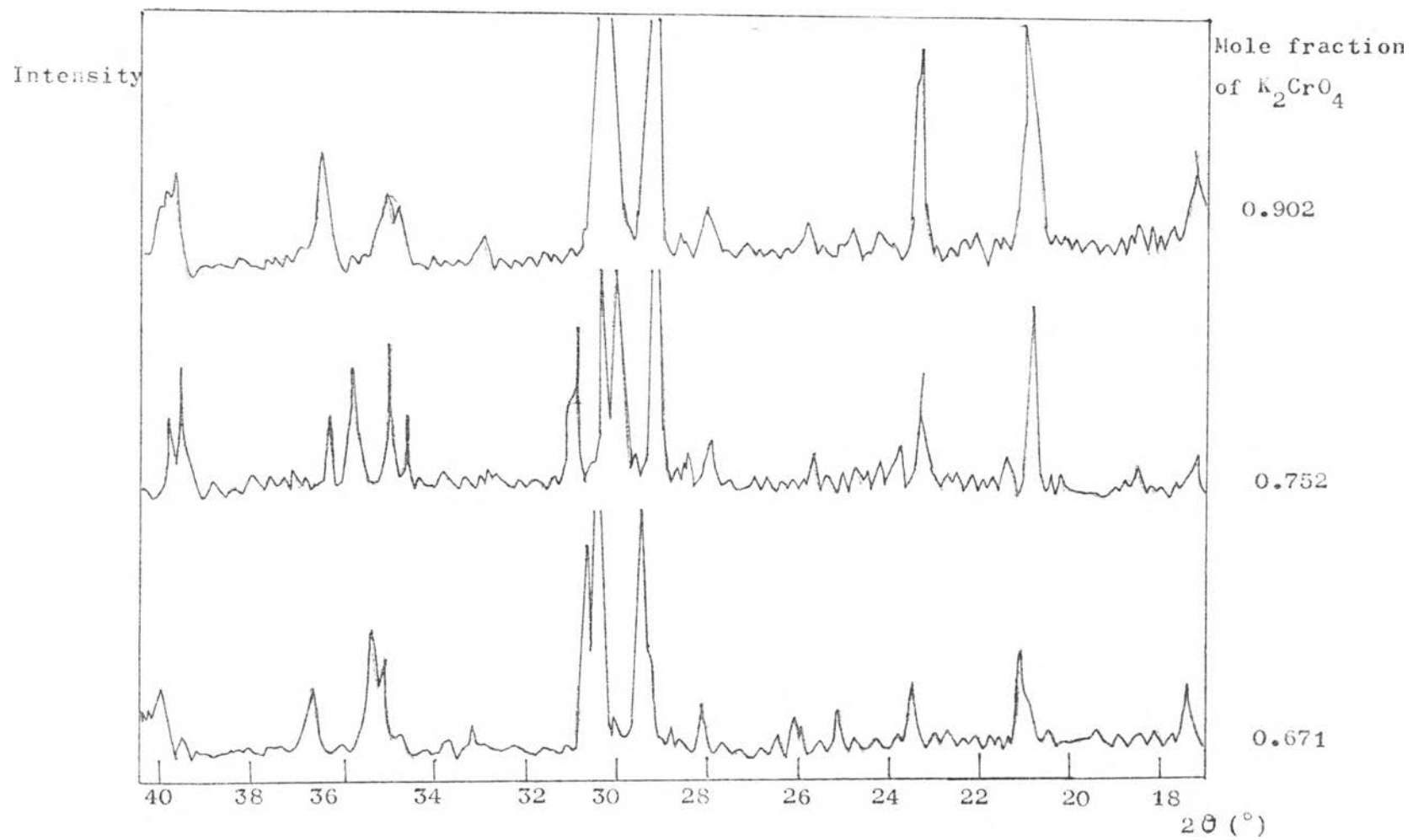


Figure 32c. The diffractograms of  $K_2CrO_4/K_2SO_4$  mixed crystals  
(cont.)

Table 46. The observed  $2\theta$  angle of potassium chromate, potassium sulphate and mixed crystals

Indices hkl	$2\theta$ angle ( $^{\circ}$ )										
	Pure $K_2CrO_4$	Pure $K_2SO_4$	$K_2CrO_4 / K_2SO_4$ mixed crystals								
			x = 0.053	0.192	0.275	0.353	0.482	0.554	0.671	0.753	0.902
			y = 0.947	0.808	0.725	0.647	0.518	0.446	0.329	0.247	0.098
020	17.10	17.60	17.60	17.60	17.55	17.50	17.40	17.30	17.20	17.10	17.10
120	20.85	21.30	21.30	21.30	21.25	21.20	21.00	20.95	20.90	20.90	20.85
200	25.30	23.80	23.80	23.70	23.65	23.60	23.50	23.45	23.40	23.35	23.30
310	25.70	26.30	26.30	26.20	26.10	26.05	26.00	25.90	25.80	25.70	25.70
201	28.60	29.20	29.20	29.20	29.00	28.90	28.85	28.80	28.75	28.70	28.60
220	29.10	29.80	29.80	29.75	29.70	29.65	29.45	29.40	29.40	29.30	29.15
031	29.92	30.80	30.80	30.75	30.70	30.65	30.40	30.30	30.20	30.05	30.00
002	30.25	31.00	31.00	30.90	30.80	30.75	30.60	30.50	30.40	30.30	30.25
221	34.55	35.60	35.60	35.60	35.55	35.45	35.35	35.20	35.05	34.65	34.60
112	35.00	36.00	36.00	36.00	35.90	35.80	35.60	35.40	35.20	35.10	35.05
040	36.25	37.80	37.80	37.80	37.55	37.65	36.70	36.80	36.60	36.30	36.30
230	36.90	38.00	38.00	38.00	37.95	37.90	37.60	37.55	37.40	37.20	36.75
122	39.45	40.40	40.40	40.40	40.35	40.30	40.25	40.00	39.80	39.60	39.50

Note x is mole fraction of potassium chromate in mixed crystals  
y is mole fraction of potassium sulphate in mixed crystals

The unit cell parameters (a, b, c) of the mixed crystals were determined by two methods; the least square method and the unique value method. The results were reported in Table 47, 48. The unit cell parameters were plotted against the mole fraction of potassium chromate in the mixed crystals in Figures 33, 34, 35.

Table 47. The unit cell parameters of mixed crystals by the least square method.

Unit cell parameter (A)	Pure $K_2CrO_4$	Pure $K_2SO_4$	Composition of mixed crystals								
			x= 0.053	0.192	0.275	0.353	0.482	0.554	0.671	0.753	0.902
			y= 0.947	0.808	0.725	0.647	0.518	0.446	0.329	0.247	0.098
a	7.587	7.220	7.220	7.231	7.236	7.252	7.260	7.267	7.273	7.321	7.375
b	9.942	9.551	9.551	9.551	9.560	9.579	9.642	9.756	9.814	9.881	9.911
c	5.954	5.810	5.810	5.828	5.848	5.851	5.866	5.882	5.896	5.899	5.900

Table 48. The unit cell parameters of mixed crystals by the unique value method.

Unit cell parameter (A)	Pure $K_2CrO_4$	Pure $K_2SO_4$	Composition of mixed crystals								
			x= 0.053	0.192	0.275	0.353	0.482	0.554	0.671	0.753	0.902
			y =0.947	0.808	0.725	0.647	0.518	0.446	0.329	0.247	0.098
a	7.628	7.468	7.468	7.502	7.519	7.536	7.564	7.582	7.599	7.610	7.628
b	10.363	10.070	10.070	10.070	10.101	10.132	10.183	10.246	10.298	10.363	10.363
c	5.903	5.764	5.764	5.784	5.800	5.811	5.838	5.858	5.875	5.893	5.903

Note x is mole fraction of potassium chromate in the mixed crystals .

y is mole fraction of potassium sulphate in the mixed crystals.

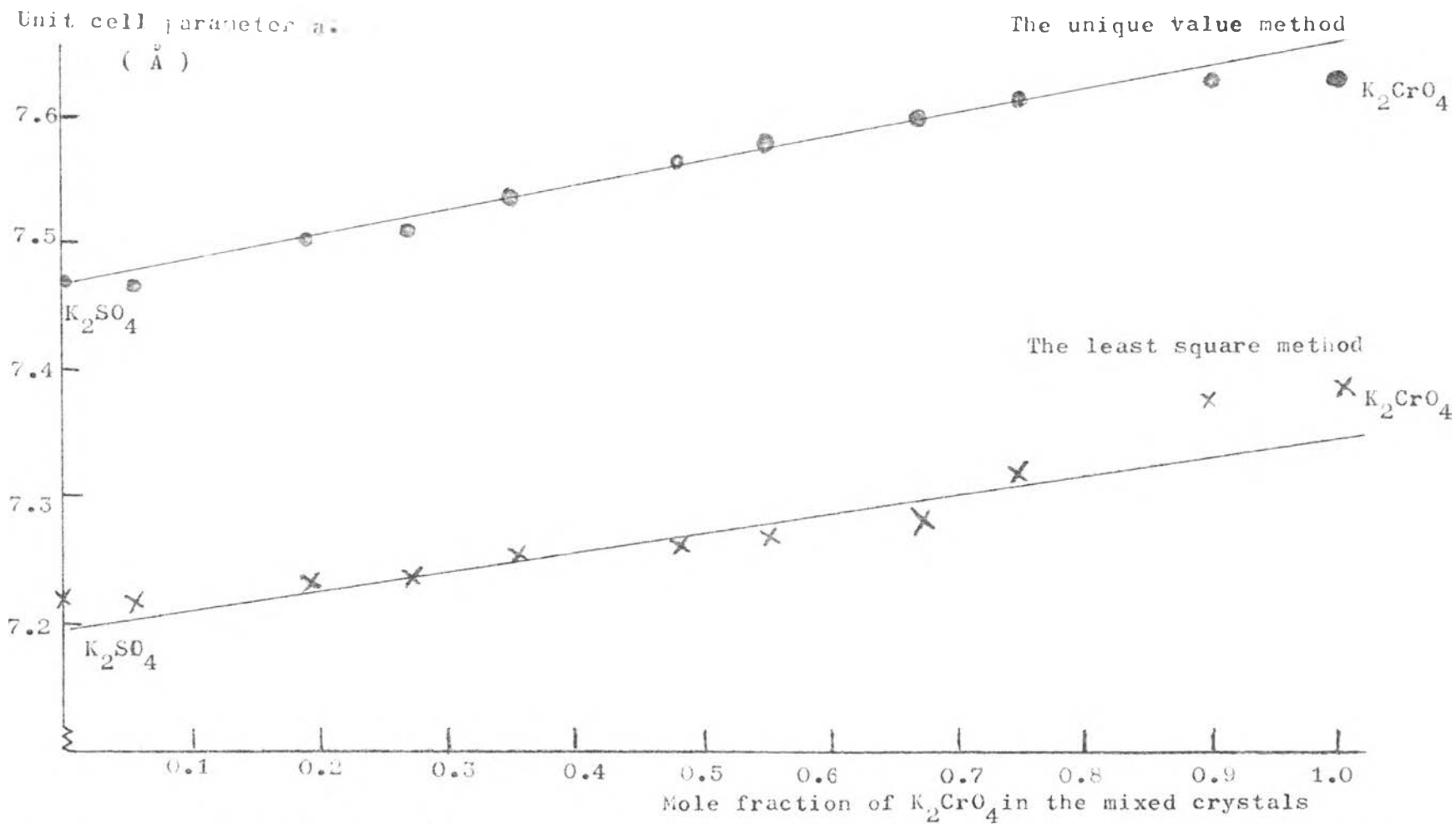


Figure 33. The graphical plot between mole fraction of potassium chromate in the mixed crystals and the unit cell parameter  $a$ .

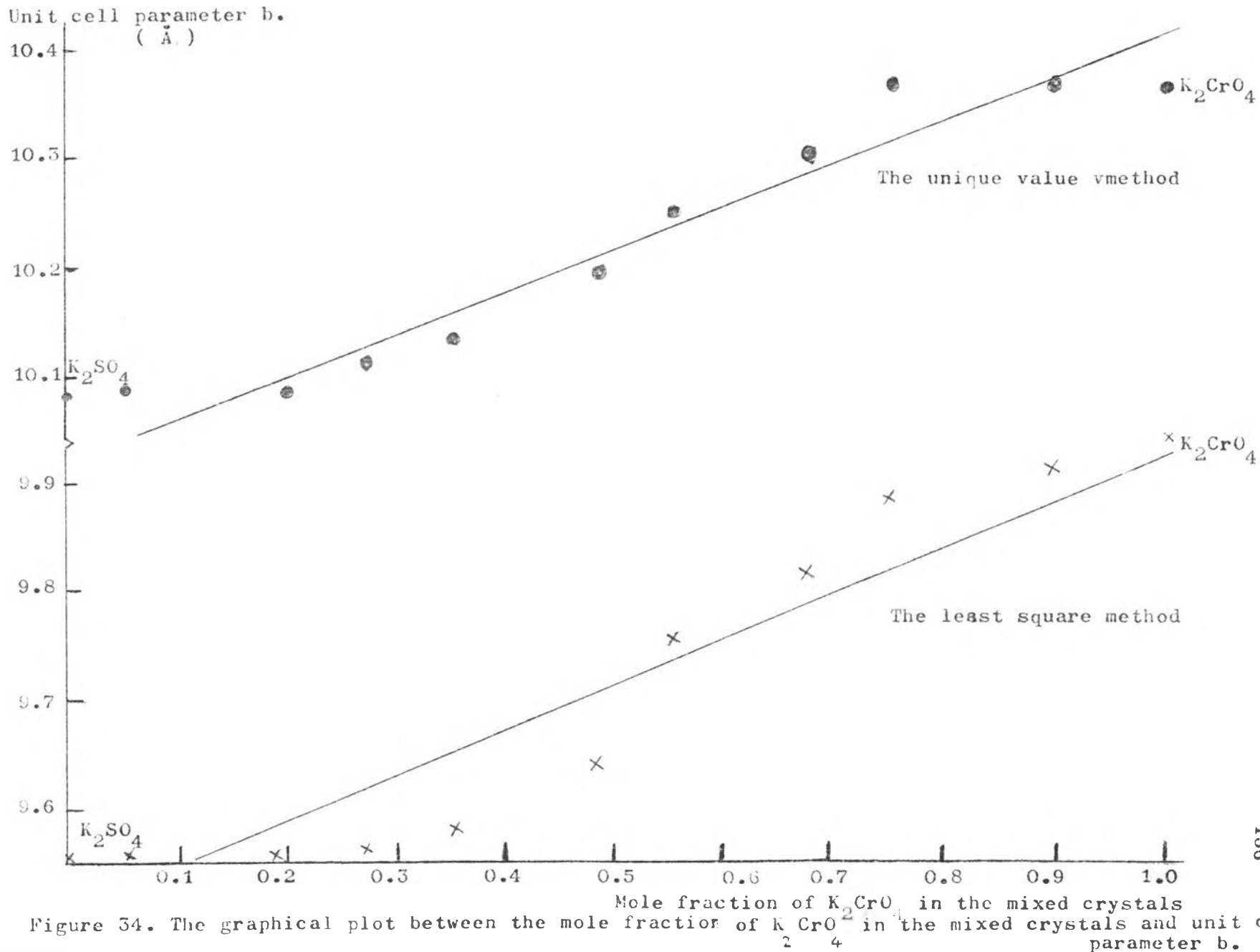


Figure 34. The graphical plot between the mole fraction of  $K_2CrO_4$  in the mixed crystals and unit cell parameter  $b$ .

Unit cell parameter c.

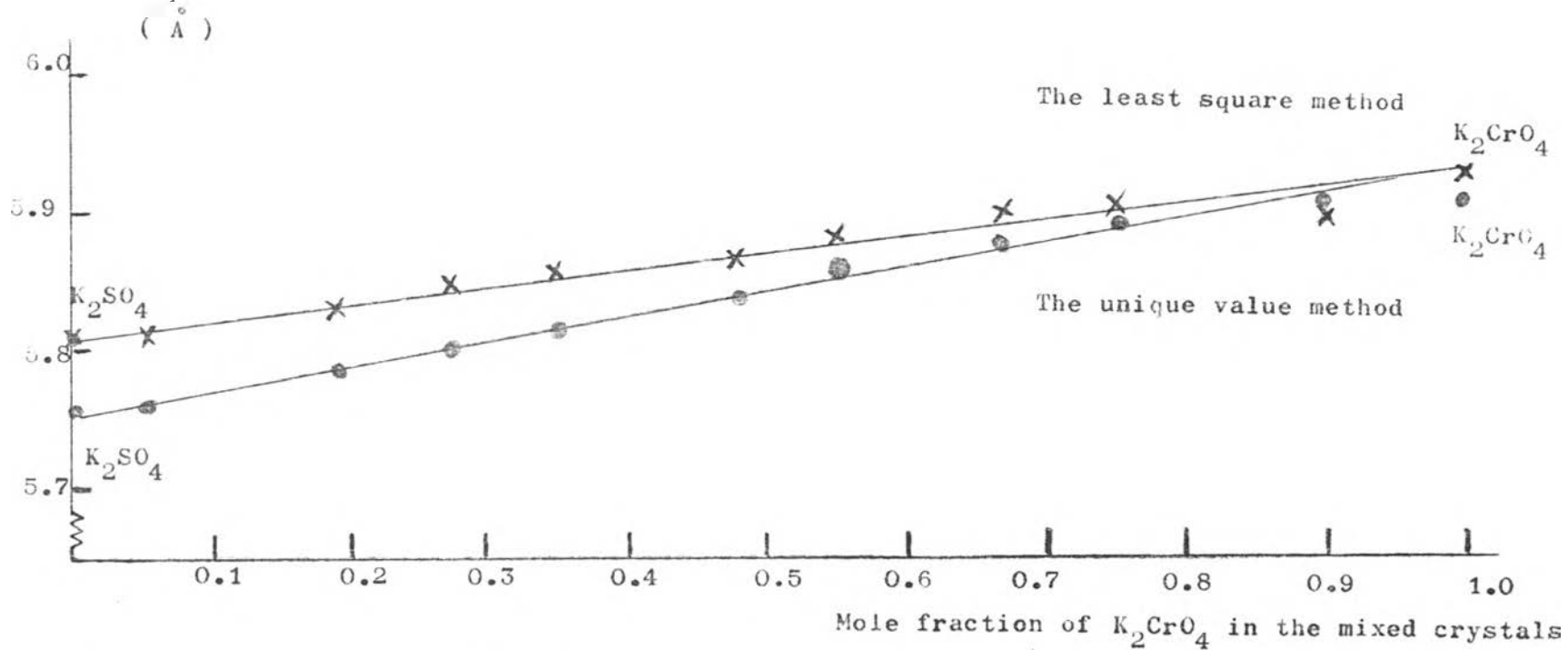


Figure 35. The graphical plot between mole fraction of  $K_2CrO_4$  in the mixed crystals and the unit cell parameter c. of the mixed crystals.



Table 48. The unit cell volumes of the mixed crystals.

% by weight		Unit cell volume ( $\text{\AA}^3$ )	
$\text{K}_2\text{CrO}_4$	$\text{K}_2\text{SO}_4$	Least square method	Unique value method
0.00	100.00	400.65	433.47
5.87	94.13	400.65	433.47
20.93	79.07	402.50	436.95
29.71	70.29	404.54	440.51
37.81	62.19	406.45	443.70
50.90	49.10	410.63	449.67
58.05	41.95	417.02	455.08
74.76	25.24	420.84	459.75
77.26	22.74	426.73	464.74
91.11	8.90	431.25	466.63
100.00	0.00	435.80	466.63

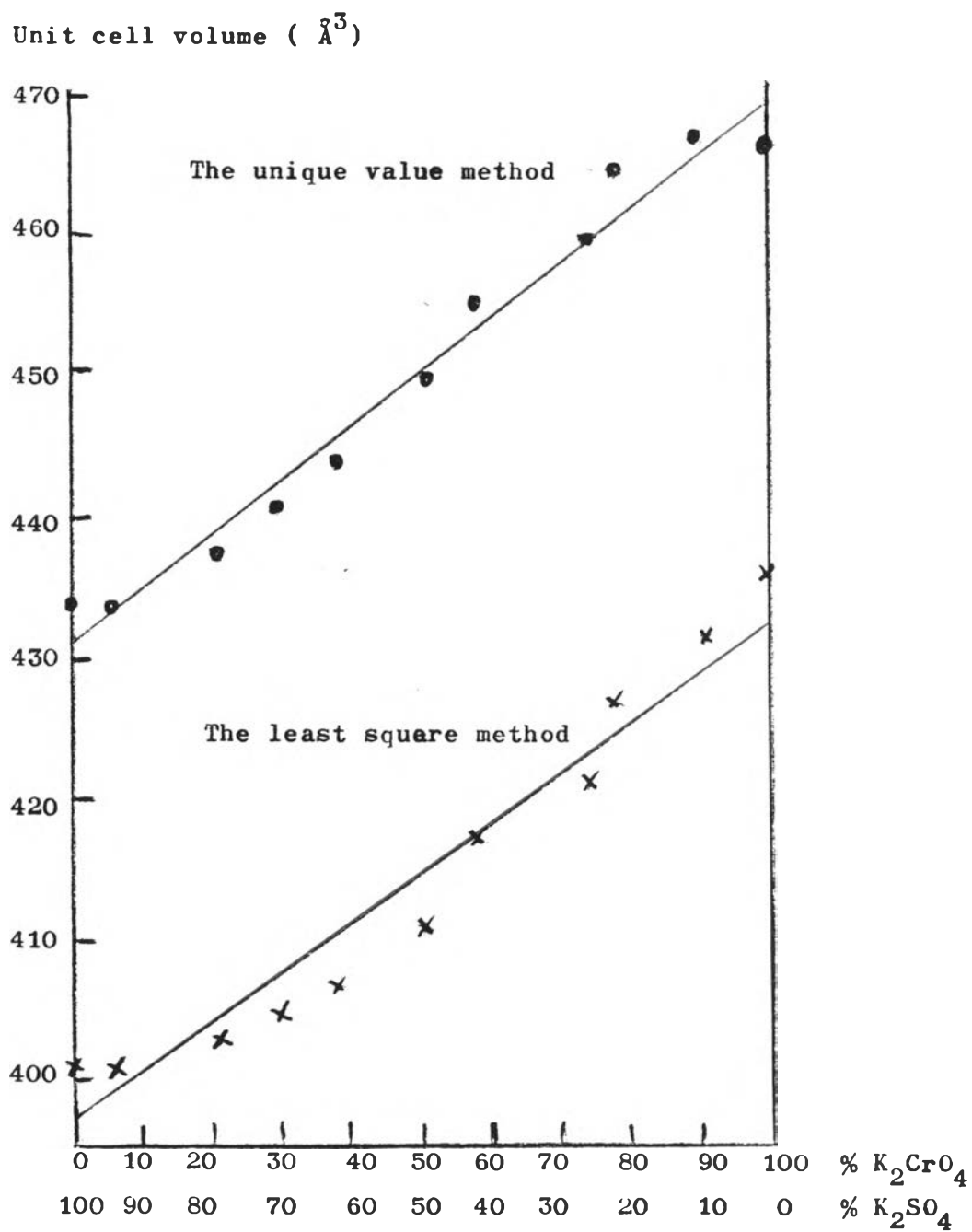


Figure 35. The graphical plot between the unit cell volumes of the mixed crystals and the compositions of the mixed crystals.

#### 4. The X-ray Powder Diffraction Data of Mixtures (Potassium Chromate and Potassium Sulphate)

The X-ray powder diffraction data of the mixtures were reported in Table 49. The diffractograms of the mixtures were also shown in Figure 36.

The diffraction patterns of the mixtures resembled a simple superposition of the diffraction patterns of the two pure crystals.

Table 49. The observed  $2\theta$  angle of the mixtures potassium chromate and potassium sulphate.

Indice hkl	$2\theta$ angle ( $^{\circ}$ )							
	Pure $K_2CrO_4$	Pure $K_2SO_4$	Mixture of $K_2CrO_4$ and $K_2SO_4$					
			$x = 0.200$ $y = 0.800$		0.560 0.440		0.878 0.122	
020	17.10	17.60	17.10	17.60	17.10	17.60	17.10	17.60
120	20.85	21.30	20.85	21.30	20.85	21.30	20.85	21.30
200	23.30	23.80	23.35	23.80	23.30	23.80	23.30	23.80
210	25.70	26.30	25.70	26.35	25.70	26.35	25.70	26.30
201	28.60	29.20	28.60	29.20	28.60	29.20	28.60	29.20
220	29.10	29.80	29.10	29.80	29.10	29.80	29.10	29.80
031	29.92	30.80	29.92	30.80	29.92	30.80	29.95	30.80
002	30.25	31.00	30.25	31.05	30.25	31.05	30.25	31.00
221	34.55	35.60	34.55	35.60	34.55	35.65	34.55	35.60
112	35.00	36.00	35.00	36.00	35.00	36.00	35.00	36.00
040	36.25	37.80	36.25	37.80	36.25	37.80	36.30	37.80
230	36.90	38.00	36.90	38.00	36.90	38.00	36.90	38.00
122	39.45	40.40	39.40	40.40	39.45	40.40	39.45	40.40

Note  $x$  is the mole fraction of  $K_2CrO_4$  in the mixtures  
 $y$  is the mole fraction of  $K_2SO_4$  in the mixtures

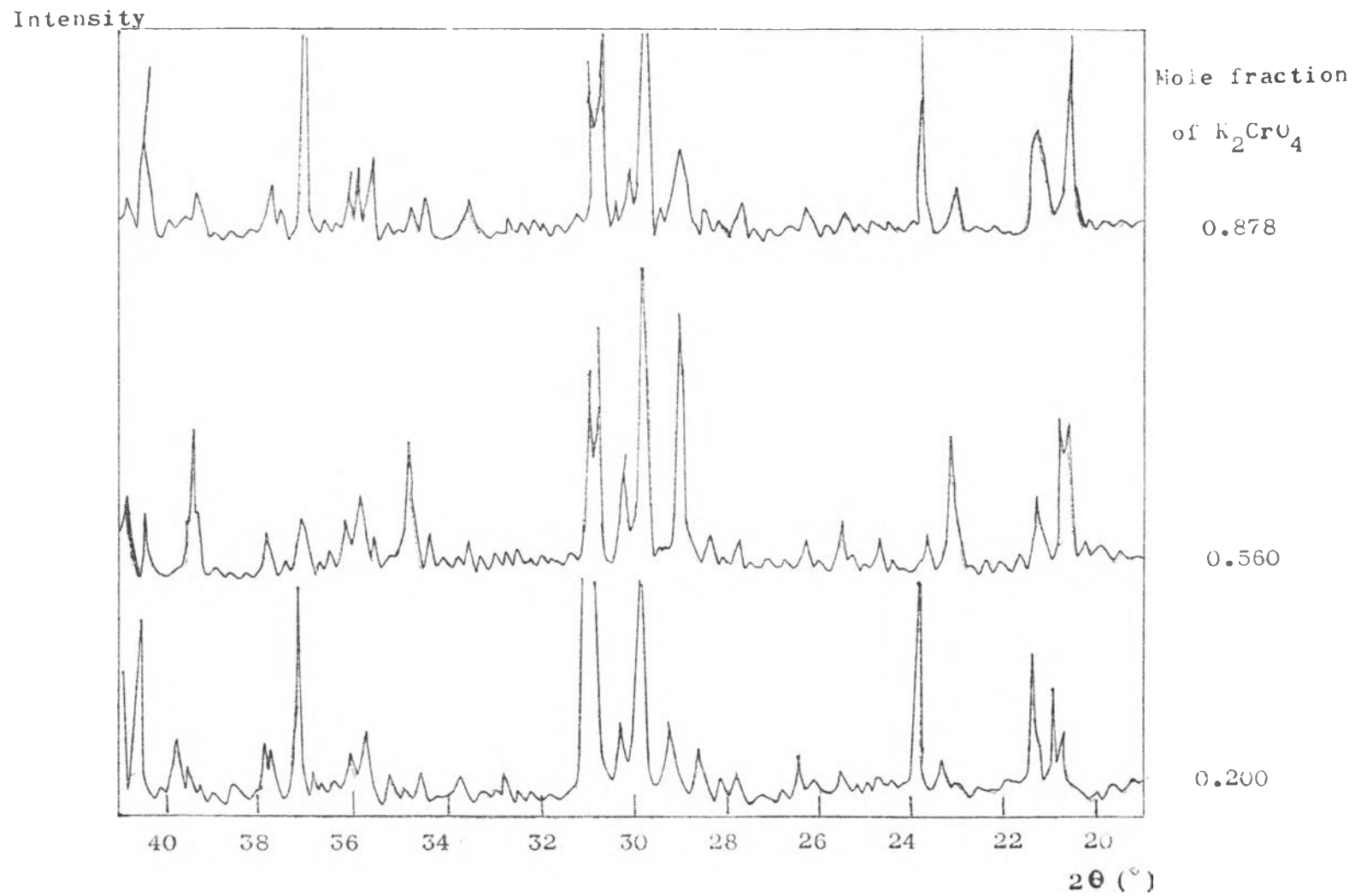


Figure 36. The diffractograms of the mixtures of potassium chromate and potassium sulphate.